https://doi.org/10.5194/acp-2021-672
Preprint. Discussion started: 31 August 2021

Atmospheric Chemistry and Physics Discussions

Field observational constraints on the controllers in glyoxal (CHOCHO) loss to aerosol

Dongwook Kim[1,2,3], Changmin Cho[2,a], Seokhan Jeong[2,b], Soojin Lee[2], Benjamin A. Nault[3,c], Pedro Campuzano-Jost[3], Douglas A. Day[3], Jason C. Schroder[3,d], Jose L. Jimenez[3], Rainer Volkamer[3], Donald R. Blake[4], Armin Wisthaler[5,6], Alan Fried[7], Joshua P. DiGangi[8], Glenn S. Diskin[8], Sally E. Pusede[9], Samuel R. Hall[10], Kirk Ullmann[10], L. Gregory Huey[11], David J. Tanner[11], Jack Dibb[12], Christoph J. Knote[13], and Kyung-Eun Min[2*]

[1]Department of Physics and Photon Science, Gwangju Institute of Science and Technology, Gwangju, South Korea
[2]School of Environmental Sciences and Environmental Engineering, Gwangju Institute of Science and Technology, Gwangju, South Korea
[3]Department of Chemistry and CIRES, University of Colorado Boulder, CO, USA
[4]Department of Chemistry, University of California, Irvine, CA, USA
[5]Institute for Ion Physics and Applied Physics, University of Innsbruck, Innsbruck, Austria
[6]Department of Chemistry, University of Oslo, Oslo, Norway
[7]Institute of Arctic and Alpine Research, University of Colorado, Boulder, CO, USA
[8]NASA Langley Research Center, Hampton, VA, USA
[9]Department of Environmental Sciences, University of Virginia, Charlottesville, VA, USA
[10]Atmospheric Chemistry Observations and Modeling, National Center for Atmospheric Research, Boulder, CO, USA
[11]School of Earth and Atmospheric Sciences, Georgia Institute of Technology, Atlanta, GA, USA
[12]Earth Systems Research Center, Institute for the Study of Earth, Oceans, and Space, University of New Hampshire, Durham, NH, USA
[13]Model-Based Environmental Exposure Science, Faculty of Medicine, University of Augsburg, Germany
[a]now at: Troposphere (IEK-8), Institute of Energy and Climate Research, Forschungszentrum Jülich, 52425 Jülich, Germany
[b]now at: Environmental Assessment group, Korea Environment Institute, Sejong, Korea
[c]now at: Center for Aerosol and Cloud Chemistry, Aerodyne Research Inc., Billerica, MA, USA
[d]now at: Colorado Department of Public Health and Environment, Denver, CO, USA

Correspondence to: Kyung-Eun Min (kemin@gist.ac.kr)

Abstract. Glyoxal (CHOCHO), the simplest dicarbonyl in the troposphere, is an important precursor for secondary organic aerosol (SOA) and brown carbon (BrC) affecting air-quality and climate. The airborne measurement of CHOCHO concentrations during the KORUS-AQ (KORea-US Air Quality study) campaign in 2016 enables detailed quantification of loss mechanisms, pertaining to SOA formation in the real atmosphere. The production of this molecule was mainly from oxidation of aromatics (59%) initiated by hydroxyl radical (OH), of which glyoxal forming mechanisms are relatively well constrained. CHOCHO loss to aerosol was found to be the most important removal path (69 %) and contributed to roughly ~20 % (3.7 μg sm^{-3} $ppmv^{-1}$ hr^{-1}, normalized with excess CO) of SOA growth in the first 6 hours in Seoul Metropolitan Area. To our knowledge, we show the first field observation of aerosol surface-area (A_{surf})-dependent CHOCHO uptake, which diverges from the simple surface uptake assumption as A_{surf} increases in ambient condition. Specifically, under the low (high) aerosol loading, the CHOCHO effective uptake rate coefficient, $k_{eff,uptake}$, linearly increases (levels off) with A_{surf}, thus, the irreversible surface uptake is a reasonable (unreasonable) approximation for simulating CHOCHO loss to aerosol.

https://doi.org/10.5194/acp-2021-672
Preprint. Discussion started: 31 August 2021


Atmospheric Chemistry and Physics Discussions

Dependency of photochemical impact, as well as aerosol viscosity, are discussed as other possible factors influencing CHOCHO uptake rate. Our inferred Henry's law coefficient of CHOCHO, 7.0×10^{8} M atm^{-1}, is ~ 2 orders of magnitude higher than those estimated from salting-in effects constrained by inorganic salts only, which urges more understanding on CHOCHO solubility under real atmospheric conditions.

1. Introduction

Glyoxal (CHOCHO), the simplest α-dicarbonyl, has significant importance in air quality and climate. Since this molecule is secondarily produced from oxidations of various biogenic (e.g., isoprene) (Li et al., 2016; Chan Miller et al., 2017) and anthropogenic (e.g., aromatics) (Volkamer et al., 2001; Nishino et al., 2010) volatile organic compounds (VOCs) with different yields, there have been many attempts to use CHOCHO to track parent VOC speciation together with formaldehyde (MacDonald et al., 2012; Kaiser et al., 2015; Chan Miller et al., 2016; Li et al., 2016; Zarzana et al., 2017, 2018). In addition, CHOCHO has also been proposed to be an important precursor for secondary organic aerosol (SOA) formation over the past few decades (Jang and Kamens, 2001; Liggio et al., 2005b; Volkamer et al., 2007), due to its high water solubility (Zhou and Mopper, 1990; Kroll et al., 2005; Ip et al., 2009; Kampf et al., 2013), oligomerization potential (Whipple, 1970; Liggio et al., 2005a; Loeffler et al., 2006; Galloway et al., 2009), and aqueous phase oxidation in cloud droplets and aerosol liquid water (Galloway et al., 2009; Volkamer et al., 2009; Ervens and Volkamer, 2010; Rossignol et al., 2014). The latter can be climate-relevant owing to the production of light absorbing brown carbon components (Powelson et al., 2014; Marrero-Ortiz et al., 2019; De Haan et al., 2020a, 2020b). Due to its importance in atmospheric processes, detailed CHOCHO loss mechanisms need to be better constrained.

CHOCHO losses by photolysis (Feierabend et al., 2009) and OH oxidation (Feierabend et al., 2008) are relatively well-known pathways compared to aerosol uptake. There have been many laboratory efforts to investigate the underlying mechanisms of CHOCHO's aerosol loss. Liggio et al. (2005a, 2005b) showed that CHOCHO aerosol uptake loss could be as important as photolysis and OH oxidation under atmospherically relevant chamber conditions, and thus it could be an important source of SOA. Further studies conducted since have shown that the CHOCHO uptake process is quite complex and depends on many variables such as acidity (Liggio et al., 2005b; Gomez et al., 2015; Shi et al., 2020), inorganic salts (Kroll et al., 2005; Kampf et al., 2013), radiation (Carlton et al., 2007; Galloway et al., 2009; Volkamer et al., 2009; Sumner et al., 2014), relative humidity (RH) (Curry et al., 2018; Gen et al., 2018; Shen et al., 2018), among others.

In the presence of inorganic salts such as ammonium sulfate (AS) and ammonium nitrate (AN), CHOCHO's solubility in aerosol increases several orders of magnitude compared to solubility in pure water, which is known as "salting-in" effect (Kampf et al., 2013). This can lead to a large fraction of CHOCHO being oxidized in the aqueous phase, thus resulting in less volatile products (Knote et al., 2014; Waxman et al., 2015; Sareen et al., 2017; Ling et al., 2020). In addition, CHOCHO was observed to have high solubility to some water soluble organic acid aerosol seeds such as fulvic acid, *l*-tartaric acid and *dl*-malic acid (Corrigan et al., 2008; Volkamer et al., 2009; Kampf et al., 2013). More recently, more

https://doi.org/10.5194/acp-2021-672
Preprint. Discussion started: 31 August 2021


Atmospheric Chemistry and Physics Discussions

complex controls such as the acceleration of CHOCHO uptake processes in the presence of other gaseous organic species have been reported (Qin et al., 2020). Overall, most of these studies have concluded that CHOCHO has a significant role in SOA formation. However, the solubility of CHOCHO in ambient condition is highly uncertain since the studies that constrained CHOCHO solubility in ambient conditions are rare.

Many recent regional and global modelling studies (Fu et al., 2008; Knote et al., 2014; Hu et al., 2017; Stadtler et al., 2018; Bates and Jacob, 2019; Liu et al., 2020; Qiu et al., 2020; Xu et al., 2020), as well as several studies constrained by in-situ field observations (Volkamer et al., 2007; Washenfelder et al., 2011; Li et al., 2016; Ling et al., 2020), have reported that CHOCHO contributes 0 to 25 % to SOA formation. This large variability resulted from the different conditions of the individual studies, focusing on different VOC precursors, biogenic (Li et al., 2016; Xu et al., 2020) vs anthropogenic (Volkamer et al., 2007; Liu et al., 2020; Qiu et al., 2020), and using different simulation tools, such as, 0-D box (Volkamer et al., 2007), Lagrangian (Washenfelder et al., 2011), and 3-D transport models (Fu et al., 2008; Knote et al., 2014; Chan Miller et al., 2016; Li et al., 2016; Chan Miller et al., 2017; Sareen et al., 2017; Hu et al., 2017; Liu et al., 2020; Qiu et al., 2020; Xu et al., 2020). These model studies were run with (Washenfelder et al., 2011) or without (Volkamer et al., 2007; Knote et al., 2014) steady-state assumption for CHOCHO, and employed different aerosol uptake treatments such as surface uptake only (Washenfelder et al., 2011; Li et al., 2016) or allowing simultaneous volume control processes (Knote et al., 2014; Ling et al., 2020).

To add more constraints on the CHOCHO contribution to SOA formation, we investigated CHOCHO partitioning to aerosols from an in-situ airborne campaign over the Korean Peninsula, where the emissions of CHOCHO-producing VOCs are highly variable. Two independent methods - a steady-state approach using a 0-D box model and a hybrid method (Knote et al., 2014) using semi-explicit aqueous chemistry together with surface uptake were used and compared for investigating more details in uptake processes of CHOCHO. From this work, we found that the simple surface uptake approximation is only applicable for low aerosol loading circumstance during the KORUS-AQ campaign. The dependence of these processes on photochemical activeness, together with evidence of insufficient understanding on CHOCHO solubility, especially in low inorganic salts condition, are discussed.

2. Materials and methods

We investigated the CHOCHO contribution to SOA formation (hereinafter, glySOA) via comparison of direct observations with an estimate from a diurnal steady-state 0-D box model, constrained by in-situ airborne precursor measurements. The magnitude of the evaluated aerosol enhancement owing to CHOCHO uptake is then compared to the results from the hybrid scheme similar to Knote et al. (2014). Details on the data treatment, model settings as well as the analysis methods follow.

In addition, aerosol data reported here are at standard temperature and pressure (273 K and 1013 hPa) condition, leading to the unit of µg sm^{-3} where sm^3 refers to the standard volume in cubic meters. Moreover, the median and interquartile range (25-75 %) were used to represent the variabilities in distributions, except as otherwise indicated.

https://doi.org/10.5194/acp-2021-672
Preprint. Discussion started: 31 August 2021


Atmospheric Chemistry and Physics Discussions

2.1 Data description

We used airborne measurements of CHOCHO, taken as part of the KORUS-AQ 2016 (KORea and United States – Air Quality study 2016), conducted from 1 May to 10 June, 2016, over South Korea, under the close collaboration among scientists from South Korea, U.S.A, and other countries to understand the local, regional, and hemispheric influences on emissions, chemistry, and air quality (Crawford et al., 2021). The entire KORUS-AQ 2016 dataset acquired from various measurement platforms (i.e., aircraft, research vessel, satellite and ground site) is available from the NASA data archive (https://www-air.larc.nasa.gov/missions/korus-aq/). The observational data used in this analysis were taken aboard the NASA DC-8 for research flights (RFs) where CHOCHO measurements are available (18 out of 20 RFs except RF # 01 and # 03, details are in Table S1 in supporting information, SI). We only focused on data that fall in the geographically confined area of the Korean peninsula and its coastal region (latitude: 34.3-38°N, longitude: 125.8-129°E), as shown in Fig. 1a, to investigate production and loss mechanisms of CHOCHO under the influence of inland sources in Korea (Peterson et al., 2019).

The list of chemical species as well as physical parameters used in our analysis, together with their measurement techniques, are summarized in Table 1. Here, we only provide brief descriptions of the CHOCHO measuring system, CAvity Enhanced Spectrometer for Atmospheric Researches (CAESAR), based on the same measurement principle and layout as the CHOCHO instrument at NOAA (National Oceanic and Atmospheric Administration) (Min et al., 2016). Air is drawn into the system via a coaxial overflow inlet (1/2" and 1/4" O.D. PFA tubing, total length: < 1.5 m) through a Teflon membrane filter (2 μm pore) to keep the optics clean and to avoid light attenuation by aerosol scattering. The 455 nm centered cavity consists of an LED as a light source, collimating optics, and high-reflection mirrors (reflectivity: 99.9973%, effective light path length: up to 12 km) enable us to quantify CHOCHO and NO_2 with zeroing error of 34 and 80 pptv for 5-second averages (2σ) and an accuracy of 5.8, and 5.0 %, respectively, using the custom-built retrieving algorithm of the DOASIS software (Kraus, 2006) (fitting range: 438 - 468 nm). To ensure the best instrumental performance, cavity calibrations were performed every 5 minutes by sequential overflows of He and zero air (30-second injection for each).

To analyze the magnitude of glySOA, we only focused on measurements below 2 km altitude which include the boundary layer in most cases, where the CHOCHO abundance was higher than CAESAR's detection limits. Also, CHOCHO data lower than zeroing error were removed to reduce uncertainty in the calculation of glySOA. In addition, to constrain the 0-D box model with DC-8 observations, 1-minute merged data (version R6, DOI: 10.5067/Suborbital/KORUSAQ/DATA01) were used for the measurement parameters with high time resolution. Meanwhile, for the species with coarser time resolution than 1-minute, (i.e., WAS data), a pseudo-1-minute data generation scheme, similar to that of Schroeder et al. (2020), was applied based on the measurements of the PTR-TOF-MS (for aromatics and isoprene) and CAMS (for other hydrocarbon compounds such as alkanes, alkenes, and alkyne) to match the timestamps; the detailed interpolation method is described in section S2, Fig. S1, and Table S2 in the SI. For the comparison of oxalate and OA, synchronized timestamps with SAGA filter measurements were used.

https://doi.org/10.5194/acp-2021-672
Preprint. Discussion started: 31 August 2021

Atmospheric Chemistry and Physics Discussions

2.2 Model description

The Framework for 0-Dimensional Atmospheric Modeling (F0AM v3.2) (Wolfe et al., 2016) was used as our tool to simulate CHOCHO with the Master Chemical Mechanism v3.3.1 (Jenkin et al., 2015 and references there in). We constrained our model with 50 chemical species and 10 physical parameters as listed in Table S2 in SI. The total number of chemical reactions considered in our model is over 11,325 with 3,742 chemical species tracked.

The model was initialized with observations from the aircraft, and the oVOCs (oxidized VOCs), including CHOCHO, were produced under co-evolving irradiation with fixed parent VOCs concentrations for a day at 1-minute time resolution. The photolysis frequencies evolve in real-time over the course of model steps, similar to other aircraft observations constrained box modeling works (Olson et al., 2006; Kaiser et al., 2016; Anderson et al., 2017; Marvin et al., 2017; Brune et al., 2018; Haskins et al., 2019; Brune et al., 2020; Souri et al., 2020). Specifically, the model was run for one full day, with updated photolysis frequencies (*j*s) every 1 hour, by implementing calculated solar zenith angle (SZA) and scaled with measured photolysis frequencies from the CAFS (CCD Actinic Flux Spectrometers).

2.3 Parametrizations of CHOCHO loss by SOA formation

From the F0AM results, the evolution of CHOCHO was calculated from the balance of production (P_{Gly}) and loss (L_{Gly}) rates, as described in Eq. (1).

$$\frac{d[Gly]_{mod}}{dt} = P_{Gly,mod} - L_{Gly,mod} \quad (1)$$

$$L_{Gly,mod} = L_{Gly+OH} + L_{Gly+hv} + L_{met} = \left(k_{Gly+OH}[OH]_{mod} + j_{Gly} + k_{dil}\right)[Gly]_{mod} \quad (2)$$

$L_{Gly,mod}$ only includes the losses of OH oxidation (L_{Gly+OH}), photolysis (L_{Gly+hv}), and physical processes to mimic deposition and dilution (L_{met}), as expressed in Eq. (2). Thus the $[Gly]_{mod}$ stands for the simulated CHOCHO concentration without aerosol loss. The loss rates of individual paths in the model were calculated as the sum of the corresponding reaction rate coefficient k_{Gly+OH} and photolysis frequency j_{Gly}, with physical mixing rate representing the dilution, deposition, and transport (k_{dil}, set as a day by following Wolfe et al., 2016).

The loss rate of CHOCHO via aerosol formation ($L_{Gly,aerosol}$) was then analytically quantified under steady-state assumptions using modeled production and loss rates of CHOCHO. CHOCHO is a short-lived intermediate oVOC with a lifetime of a few hours (even without considering the aerosol loss path, see Sect. 3.3), thus, the steady-state assumption is valid except for measurements near sources. Under the steady-state assumption, the production rates of CHOCHO ($P_{Gly,mod}$), directly extracted from F0AM, need to be balanced with real loss rates of CHOCHO ($L_{Gly,real}$), accounting for $L_{Gly,aerosol}$, as Eq. (3) shows.

$$P_{Gly,mod} \approx L_{Gly,real} = \left(k_{Gly+OH}[OH]_{mod} + j_{Gly} + k_{dil}\right)[Gly]_{obs} + L_{Gly,aerosol} \quad (3)$$

Here, the instantaneous OH oxidation, photolysis, and meteorological losses ($k_{Gly+OH}[OH]_{mod} + j_{Gly} + k_{dil}$) were inferred from modeled outputs as $L_{Gly,mod}/[Gly]_{mod}$. $[Gly]_{obs}$ refers to the measured CHOCHO concentration.

https://doi.org/10.5194/acp-2021-672
Preprint. Discussion started: 31 August 2021

Atmospheric Chemistry and Physics Discussions

$$L_{Gly,aerosol}=P_{glySOA,\ eff.\ Steady\ State}=P_{Gly,mod}-\left(k_{Gly+OH}[OH]_{mod}+j_{Gly}+k_{dil}\right)[Gly]_{obs}=k_{eff,uptake}[Gly]_{obs} \quad (4)$$

One should note that the CHOCHO uptake rate coefficient assessed as in Eq. (4) is regarded as a pseudo-first order, effective uptake rate coefficient ($k_{eff,uptake}$), which is a net result of competition between reversible and irreversible processes in real atmosphere. This stems from the underlying mechanisms of CHOCHO uptake on the aerosol either being reversible or not, which depends on various factors, such as aerosol acidity, seed type, RH and radiative flux, etc (Liggio et al., 2005a, 2005b; Kroll et al., 2005; Corrigan et al., 2008; Kampf et al., 2013; Curry et al., 2018).

Then, the SOA production rate, owing to CHOCHO uptake (P_{glySOA}), was estimated from the inferred $k_{eff,uptake}$ and observed CHOCHO concentration. In Sect. 3.6, we tracked the importance of P_{glySOA} in organic aerosol (OA) growth as the air mass evolves with the photochemical age, ($Photo_{age}$, hr), based on the NO_x/NO_y chemical clock, by following Kleinman et al. (2003), via Eq. (5).

$$Photo_{age}=ln\left(\frac{[NO_x]}{[NO_y]}\right)/(k_{OH+NO_2}[OH]) \quad (5)$$

Here, an updated reaction rate coefficient of OH and NO_2, 9.2×10^{-12} cm^3 $molecule^{-1}$ s^{-1}, was used (Mollner et al., 2010). For more relevant photochemical age in Korea, the average OH concentration ($5.05\pm1.82\times10^6$ molecules cm^{-3}, roughly 3-4 times higher since the measurements were conducted only in day time period, 8:00-17:00 LT) in Seoul Metropolitan Area (SMA, highest population density in Korea) during KORUS-AQ was also used.

To reconcile the deviation of diurnal steady-state assumption against the reality, photochemical age-dependent adjustment analysis was also carried out to account for the potential underestimation or overestimation in oVOCs production with respect to the plume age. Fresh plumes close to the sources tend to have not enough time for oxidation products to build up as the simulation of a full-day evolution. Meanwhile, old plumes tend to be over-processed than just one day. For that, an adjustment factor was introduced from the relationship between the ratio of modelled and measured HCHO against $Photo_{age}$. This adjustment was applied to the CHOCHO production rate; more details on the discussions and results are in section S3 and Fig. S2 to S4. The main results with this adjustment are presented together with that of the original simulation without this adjustment.

2.4 Semi-explicit estimation of CHOCHO loss to aerosol

To provide more constraints on aqueous phase reactions once CHOCHO is taken up by aerosol as well as to test the validity of our steady-state assumption in glySOA estimation, a hybrid approach, via semi-explicit aerosol loss treatment of volume processes together with surface uptake treatment, was conducted similar to Knote et al. (2014) (section S9). Details on the backgrounds and parameterizations are described in Knote et al. (2014). Briefly, for the surface processes, first-order reactive uptake treatment was used to compare with F0AM results, under the assumption of irreversible surface reaction in free molecular regime without Fuch-Sutugin correction (Tang et al., 2015; Seinfeld and Pandis, 2016) which corrects for slip correction in the transition regime. This is not only due to its negligible influence (< 5 % difference in $k_{surf,uptake}$) but also due to retain the-linear relation between $k_{surf,uptake}$ and reactive CHOCHO uptake coefficient ($\gamma_{Gly,uptake}$), as described in Eq. (6).

https://doi.org/10.5194/acp-2021-672
Preprint. Discussion started: 31 August 2021


Atmospheric Chemistry and Physics Discussions

$$k_{\text{eff,uptake}} = \frac{1}{4} v_{\text{Gly}} \gamma_{\text{Gly,uptake}} A_{\text{surf}} \quad (6)$$

Here, A_{surf} refers to the aerosol surface area density ($\text{cm}^2\ \text{cm}^{-3}$), v_{Gly} stands for the mean molecular speed ($\text{cm}\ \text{s}^{-1}$), and $\gamma_{\text{Gly,uptake}}$ (unitless) indicates the uptake probability of a CHOCHO molecule colliding and reacting on an aerosol surface. For simulating volume-controlled processes through aqueous-phase reactions, it was assumed that gas-phase and dissolved-phase CHOCHO (CHOCHO monomer, hydrates, and oligomers) are in steady-state (more details in section S4 and Fig. S6 in SI). Briefly, the equilibrium concentration of aqueous phase CHOCHO, including both hydrates and oligomers, was calculated using effective Henry's law coefficient, $K_{\text{H,eff\_Gly}}$, as in Eq. (7) from Kampf et al. (2013), and reflecting the parameterization from Waxman et al. (2015) with the kinetic limit of "salting-in" effect at high salt concentration.

$$K_{\text{H,eff\_Gly}} = \frac{K_{\text{H,water}_{\text{Gly}}}}{10^{-0.24\times \min(12, C_{\text{AS}}) - 0.07\times C_{\text{AN}}}} \quad (7)$$

Here, the parameters in parenthesis stand for the adjustment factor for $K_{\text{H,water\_Gly}}$, Henry's law coefficient of CHOCHO in dilute water. C_{AS} and C_{AN} denote the molarities (mol kg^{-1}, *m*) of AS and AN in aerosol, respectively. In this study, salting constants of 0.24 and 0.07 were applied for AS and AN, respectively, by following Waxman et al. (2015). In addition, the kinetic limit of 12 *m* was set only for the concentrations of AS (Kampf et al., 2013), since that of AN has not been experimentally demonstrated yet.

For the instantaneous equilibrium partitioning between CHOCHO monomers and oligomers, an oligomerization constant (K_{olig}=$[\text{Gly}]_{\text{oligomer}}$/$[\text{Gly}]_{\text{monomer+hyrate}}$) of 0.5 (1) was used for the cases where C_{AS} is larger (smaller) than the limit of salt concentration, 12 *m* (Knote et al., 2014). In addition, aqueous phase OH oxidation path was treated as an effective photochemical reaction with the rate of CHOCHO monomer and hydrates ($k_{\text{photochem}}$, 2 s^{-1}) adopted from Ervens and Volkamer (2010), since $[\text{OH}]_{\text{aq}}$ inferred from measured gas-phase OH under the assumption of equilibrium state ($K_{\text{H,OH}}$ = 25 M atm^{-1}) (Klaning et al., 1985) is highly uncertain; estimated $[\text{OH}]_{\text{aq}}$ with $K_{\text{H,OH}}$ does not only account for losses of OH in aerosols (Herrmann et al., 2010; Waxman et al., 2013) but also for additional radical generation from photochemical reactions of organics (Volkamer et al., 2009; Monge et al., 2012; Tong et al., 2016) and inorganics (Paulson et al., 2019).

Aerosol physical sizes measured from LARGE (Langley Aerosol Research Group Experiment) are dried aerosol sizes. To estimate the ambient diameter of an aerosol, and thus estimate more realistic aerosol surface area density, the hygroscopic growth factor (gf_{diam}) following Brock et al. (2016) was used as described in Eq. (8).

$$gf_{\text{diam}} \cong \left(1 + \kappa_{\text{chem}} \times \frac{\text{RH}}{\text{100-RH}}\right)^{1/3} \quad (8)$$

Here, the hygroscopicity parameter (κ_{chem}) for a mixed particle was calculated from the volume-weighted average of its individual chemical components (OA, NH_4NO_3, $(NH_4)HSO_4$ and $(NH_4)_2SO_4$) and most of the hygroscopicity were taken from Brock et al. (2016) and references therein, but OA. The hygroscopicity parameter of OA (κ_{OA}) was parameterized with O/C as 0.190×(O/C)-0.0048 by following Rickards et al. (2013).

C_{AS} and C_{AN} in Eq. (8) are calculated from the sulfate, nitrate and aerosol liquid water content (ALWC) calculated from Extended Aerosol Inorganic Model (E-AIM) (Clegg and Brimblecombe, 1990; Clegg et al., 1998; Massucci et al.,

https://doi.org/10.5194/acp-2021-672
Preprint. Discussion started: 31 August 2021


Atmospheric Chemistry and Physics Discussions

1999; Wexler, 2002; Friese and Ebel, 2010). In the model, the amount of each chemical component in aerosol was calculated from the measurements of gas-phase HNO_3, particle-phase ammonium, nitrate, and sulfate as well as local environmental parameters (e.g., RH and temperature). Inorganic aerosol mass from the AMS and gas-phase HNO_3 from CIT-CIMS were used to run the E-AIM model (specifically, Model IV, in forward mode with ammonia being estimated recursively) (Clegg et al., 1998; Friese and Ebel, 2010). ALWC associated with inorganic compounds was also calculated from the E-AIM model. When calculating ALWC, organic portion was added if O/C (oxygen to carbon ratio of OA) was higher than 0.7, assuming organic phase separation from inorganics at O/C less than 0.7 (Song et al., 2018, 2019; Gorkowski et al., 2020).

3. Results and discussion

3.1 Observed spatial distribution of CHOCHO and relevant species

The average CHOCHO concentration over the whole campaign period was 107 ± 58 ppt, with the highest concentration of 1.05 (2.10) ppb for 1 minute (10 second) average. The spatially binned (latitude: 0.14°, longitude: 0.15°) CHOCHO distribution, together with other relevant measured species, as well as the DC-8 flight tracks, are shown in Fig. 1. In general, the concentrations of the enhanced CHOCHO and other species were observed near the SMA and the West Coastal Industrial Area (WCIA) where petrochemical complex, steel mill, and power plant facilities are located. The observed CHOCHO enhancement is comparable to previously reported airborne measurements taken over the southeastern United States (up to 1.0 ppb within boundary layer) (Li et al., 2016). The spatial distribution of CHOCHO (Fig. 1b) is somewhat different from other oVOCs, specifically, HCHO, another ubiquitous oVOC (Fig. 1c). The CHOCHO enhancement over the WCIA is less comparable to CO than that of HCHO, where VOCs such as ethane, propane, ethene, and n-butane emissions are dominant in this region (Simpson et al., 2020). Meanwhile, aromatic distributions have more similarities with CHOCHO, such as toluene (Fig. 1f), xylene, and trimethylbenzenes near SMA (Fig. S7).

3.2 0-D box model results

Figure 2 shows the direct comparisons of chemical species estimated from the F0AM to the measurements taken on board. Unless otherwise specified, the least-orthogonal-distance regression (ODR) forced through zero intercept method is used for linear regression fits and Pearson R is for the goodness of the fits. In general, the diurnal steady-state box model simulates the gas-phase oxidation processes reasonably well considering the measurement uncertainties as shown for OH, HO_2, and HCHO (Fig. 2a-c). In contrast to HCHO, where the model shows broad agreement (an overall slope of 1.23 ± 0.02), the CHOCHO model overestimates by 3.24 (± 0.06) times (Fig. 2d). For the model run without photochemical age dependent adjustment, HCHO and CHOCHO regression slopes are 1.08 (± 0.01, Fig. S2c-d) and 2.89 (± 0.05). This model-observation discrepancy of CHOCHO was also observed in other urban environments such as Mexico City (Volkamer et al., 2007) and the Pearl River Delta (Ling et al., 2020).

https://doi.org/10.5194/acp-2021-672
Preprint. Discussion started: 31 August 2021


Atmospheric Chemistry and Physics Discussions

We presume that our model overestimation is due to underestimation in CHOCHO loss, since the CHOCHO instrumental loss along the airway had been identified as negligible (0.0001±0.005 $cm^2 s^{-1}$ %) (Min et al., 2016) and oVOC production in the model is comparable to that of reality; the modelled OH reactivity is only 8 % (on average) higher than measurements (Fig. S5d), in addition to the fact that the constrained parent VOCs from the combined observations of WAS, PTR-TOF-MS, and CAMS were quite comprehensive.

Moreover, the direct comparison between modelled and measured CHOCHO neglects the possible contribution of primary CHOCHO emission in the measurements. Qiu et al. (2020) showed the importance of primarily emitted CHOCHO in Beijing in a wintertime study, finding direct CHOCHO emissions from vehicles and industrial activities. Since we assumed that all measured CHOCHO was secondarily formed, we cannot rule out the possibility of an even larger discrepancy in model and observation, especially for the SMA and industrial area where direct CHOCHO emission is suspected to be not negligible. We prefer to provide a conservative glySOA by assuming all measured CHOCHO to be secondary, since the portion of primary CHOCHO in aircraft measurements is largely uncertain. However, considering vertical transport time with respect to the short lifetime of CHOCHO, most of the measured CHOCHO aboard is expected to be secondary.

To test the hypothesis that the gap between modelled and observed CHOCHO can be explained by uptake to aerosol, a steady-state approach was used (as described in Sec. 2.3) to infer $k_{eff,uptake}$. As a quality check, we plugged $k_{eff,uptake}$ parameter back into the model to simulate the loss of CHOCHO via glySOA path. The CHOCHO prediction with updated loss to aerosol reproduced measured CHOCHO well, as shown in Fig. 2d, thus we presume that the possible bias of primary CHOCHO contribution is not significant. Possible bias in $k_{eff,uptake}$ due to the measurement errors was quantified by varying input concentrations with their uncertainties. As shown in Fig. S8 in section S6, the largest variability in VOCs input results in ±10 % variation of $k_{eff,uptake}$. In addition, the possible errors in photochemical age dependent adjustment are about 27 %, as shown in Fig. S4. More about the controlling factors in $k_{eff,uptake}$ follows in section 3.4 after the sources and sinks discussion.

3.3 CHOCHO sources and sinks apportionment

Roughly 59 % of CHOCHO in the model originates from aromatics, with the largest contribution from toluene (41 %, Fig. 3a). We estimate that 20 % of CHOCHO is produced from biogenic VOCs (BVOCs), specifically isoprene and α-, β-pinene. However, we cannot rule out possible underestimation in fast oxidized BVOCs contribution since we initialized our model with measurement aboard than emission rates or surface measurements.

The OH oxidation and photolysis loss are responsible only for 13 and 19 % of CHOCHO losses, respectively, while roughly 69 % of CHOCHO must be lost via aerosol uptake to reconcile the imbalance between modelled and measured concentration (Fig. 3b). This large importance of the aerosol uptake pathway is consistent with previous works in Mexico City (75-95 %) (Volkamer et al., 2007) and in the Pearl River Delta measurements (~ 62 %) (Ling et al., 2020), while much larger than that in Los Angeles (0-30 %) (Washenfelder et al., 2011).

https://doi.org/10.5194/acp-2021-672
Preprint. Discussion started: 31 August 2021


Atmospheric Chemistry and Physics Discussions

The model-estimated lifetime of CHOCHO, 1.57 ± 0.23 hours, without aerosol uptake (in Fig. S9), is consistent with the general estimation of a few hours. However, when aerosol uptake is included, the CHOCHO lifetime decreases to 0.50 ± 0.26 hours during the typical flight duration (8:00 – 17:00 LT), which is also consistent with previous results (Volkamer et al., 2007).

The importance of aerosol uptake loss has clear dependence on A_{surf}. Figure 3c shows the ratio of $k_{eff,uptake}/(k_{OH+Gly}[OH]+j_{Gly})$ against A_{surf}. This ratio levels off around 2.5 under high A_{surf} condition but it converges to 0 as A_{surf} decreases since the $k_{eff,uptake}$ becomes close to 0 under no aerosol condition (no significant positive intercept) as shown in Fig. 4a. This confirms that our inferred $k_{eff,uptake}$ is legitimate, since the CHOCHO budget is closed only with photolysis and OH oxidation loss in the absence of aerosol. Meanwhile, our steady-state model diverges more, and thus required higher $k_{eff,uptake}$ to reconcile the gap with observed CHOCHO as A_{surf} increases. This is a clear evidence of required additional sink of CHOCHO which is linked with aerosol abundance.

3.4 Different CHOCHO uptake regimes

The estimated $k_{eff,uptake}$ is 1.2-6.0×10^{-4} s^{-1} throughout the whole mission which falls within the range of previous reports (1.3 – 5.0×10^{-4} s^{-1}) (Hastings et al., 2005; Liggio et al., 2005a; Ervens and Volkamer, 2010). Interestingly, our inferred $k_{eff,uptake}$ has clear dependency on A_{surf} as shown in Fig. 4a. The $k_{eff,uptake}$ shows a linear relationship with A_{surf} in lower A_{surf} condition (less than 4.9×10^{-6} cm^2 cm^{-3}, with averaged ν_{Gly}, 3.3×10^4 cm s^{-1}, hereafter defined as Regime I). Meanwhile, $k_{eff,uptake}$ levels off for larger A_{surf} (hereafter named as Regime II). One should note that slopes in this figure become the reactive uptake coefficient, $\gamma_{Gly,uptake}$, since it shows the relation between $k_{eff,uptake}$ and A_{surf} scaled with 1/4 ν_{Gly}. Extracted median $\gamma_{Gly,uptake}$, assuming 100% surface uptake, are 0.98 (±0.07)×10^{-2} for Regime I, and 0.82 (±0.57)×10^{-2} for both regimes which also overlap with what Ervens and Volkamer (2010) reported for hygroscopic aerosol (0.8±0.3×10^{-2}).

The linearity between $k_{eff,uptake}$ and A_{surf} in Regime I indicates that irreversible uptake on the aerosol surface is a reasonable approximation to mimic the behaviour of CHOCHO uptake for the conditions with low aerosol loading, since averaged aerosol modes across the regimes are found to be similar with each other over varying A_{surf} (Fig. S10), thus the number of particles matters more than aerosol size.

As shown in Fig. 4b, the $k_{eff,uptake}$ dependence on j_{NO2} (a proxy for solar irradiation), exists in both regimes (more apparent in Regime II, where $k_{eff,uptake}$ enhanced by ~ 40 % at higher j_{NO2}, compared to lower j_{NO2}) and suggests the possibility of accelerated aqueous phase chemistry in SOA under active photochemistry. This light dependence of $k_{eff,uptake}$ is consistent with findings from previous laboratory studies as significant acceleration in CHOCHO aerosol uptake under irradiated (compared to dark) conditions (Volkamer et al., 2009; Ervens and Volkamer, 2010). We speculate the effect of low volatile compounds' coatings on aerosols seed may not have played a significant role in our environment (Galloway et al., 2011). The increase in $k_{eff,uptake}$ (decrease in CHOCHO uptake time scale) under high j_{NO2} may reflect faster production of low volatility products via irreversible pathways, likely due to enhanced organic photochemistry (Volkamer et al., 2009; Lee et al., 2011).

https://doi.org/10.5194/acp-2021-672
Preprint. Discussion started: 31 August 2021


Atmospheric Chemistry and Physics Discussions

In Regime II, $k_{eff,uptake}$ plateaus in a range of 3-6×10^{-4} s^{-1} and becomes relatively insensitive to A_{surf}. One possible explanation of independent behavior of $k_{eff,uptake}$ in Regime II is likely related to aerosol viscosity. Figure 4c shows C_{AS} and C_{AN} change with respect to A_{surf}; C_{AN} increases and levels off near the boundary of Regime I and II. An increase in salt content will lead to highly viscous aerosol, and thus retards mass transfer into the aerosol. Kampf et al. (2013) previously observed slower CHOCHO mass transfer for C_{AS} larger than 12 *m* condition. Similar behavior is expected for C_{AN}, thus, more studies on C_{AN} effect on the time scale of CHOCHO mass transfer into particle are desired.

3.5 glySOA production rate comparison

Figure 5 (a) shows the results of glySOA production rate (P_{glySOA}) comparison between 0-D box model ($P_{glySOA, eff. Steady State}$, Eq. 4) and hybrid treatment ($P_{glySOA, hybrid}$, Sect. S9) in Regime I. Calculated P_{glySOA} without surface uptake (volume process only) is 2-3 orders of magnitude slower than that of the steady-state result, suggesting the importance of surface uptake process in Regime I, which is consistent with previous model studies (Ervens and Volkamer, 2010; Knote et al., 2014). By adding surface uptake process, using the median $\gamma_{Gly,uptake}$ in Regime I (0.98 ×10^{-2}), the hybrid method matches within an order of magnitude with steady-state box model analysis.

In Regime II, where reactive surface uptake process is unlikely due to the lack of linearity between $k_{eff,uptake}$ and A_{surf} (Fig. 4a-b), inferred P_{glySOA} from constrained K_{H,eff_Gly} with measured C_{AS} and C_{AN} through Eq. (7) without surface uptake process ($P_{glySOA, eff. photochem}$, Sect. S4) is 2 orders of magnitude lower than $P_{glySOA, eff. Steady State}$ as shown in colored circles in Fig. 5b. One fixed K_{H,eff_Gly} of 7.0×10^{8} M atm^{-1}, close to the K_{H,eff_Gly} at AS seed kinetic limit (~3×10^{8} M atm^{-1}, Kampf et al., 2013) provides better agreement. It indicates that the K_{H,eff_Gly} driven by AS and AN is not sufficient enough to explain the required K_{H,eff_Gly} of CHOCHO. Although the increase in CHOCHO solubility by some of the inorganics other than AS and AN not included in K_{H,eff_Gly} calculation (e.g., NaCl and NH_4HSO_4) cannot be ruled out, due to their low concentrations, the K_{H,eff_Gly} contribution from these species is not significant enough (less than 5 %) to explain the required K_{H,eff_Gly}. Even higher K_{H,eff_Gly} (3×10^{9} M atm^{-1}) is required for Regime I (Fig. S11).

One possible explanation for high K_{H,eff_Gly} (~10^{8} M atm^{-1}) even in low salt conditions (i.e., C_{AS}<12 *m*) is the influence of organic compounds by various oligomerization pathways. Moreover, aerosol seeds consist of water-soluble organic carbons (e.g. fulvic acid) can enhance the solubility of CHOCHO (up to ~6.0×10^{8} M atm^{-1} of K_{H,eff_Gly}, Volkamer et al., 2009). Corrigan et al. (2008) observed K_{H,eff_Gly} > 10^{8} M atm^{-1} with various organic acid aerosol seeds, including *l*-tartaric acid, *dl*-malic acid, and other liquid-phase aerosol particles containing amine functional groups. In addition, Qin et al. (2020) found the synergetic effect of CHOCHO uptake by coexistence with pinanediol and proposed acid-catalyzed cross-reactions which enhance the reactivity of CHOCHO in the aqueous phase.

3.6 CHOCHO contribution to SOA in SMA

To evaluate CHOCHO contribution to SOA formation in SMA, the relationship between P_{glySOA} and organic aerosol enhancement (ΔOA) normalized with ΔCO for minimizing dilution effect, was analyzed along with the air mass evolution

https://doi.org/10.5194/acp-2021-672
Preprint. Discussion started: 31 August 2021


Atmospheric Chemistry and Physics Discussions

(Fig. 6), where the background concentrations of OA and CO are 1 μg sm^{-3} and 140 ppb, respectively, as for Yellow Sea case in Nault et al. (2018). The $P_{glySOA}/\Delta CO$ increases as an average of 3.67 μg sm^{-3} ppm^{-1} hr^{-1} for the first 6 equivalent hours under 4.84×10^{6} molecules cm^{-3} OH (averaged OH concentration over SMA) and the rate of $\Delta OA/\Delta CO$ growth over that time window is 17.3 μg sm^{-3} $ppmv^{-1}$ hr^{-1}. Thus, the CHOCHO contribution to SOA formation during the early stage of photochemical processing is estimated to be ~20 %. During the KORUS-AQ, the observationally constrained P_{glySOA} ranges from 0-0.8 μg sm^{-3} hr^{-1} for individual RFs (shown in Fig. S12 in SI), which is comparable to Mexico City (> 15 %, Volkamer et al., 2007), Pearl River Delta (11.3 %, Ling et al., 2020) and Los Angeles basin (1-15 %, Knote et al., 2014) but higher than Pasadena (0-4 %, Washenfelder et al., 2011).

We also estimate the upper limit of oxalate mass yield from CHOCHO over SMA as ~ 10 % based on the oxalate fraction (~2 %) in OA (Fig. 6c). Our analysis shows lower oxalate yield than previously reports from the OH oxidation in cloud process (Tan et al., 2009, Lim et al., 2013; Ortiz-Montalvo et al., 2014). We presume our lower yield has likely originated from the existence of many fates in uptaken CHOCHO, such as oligomerization (Lim et al., 2013), reaction with sulfate (Lim et al., 2016) and ammonium (Yu et al., 2011; Ortiz-Montalvo et al., 2014), etc., since our analysis is over SMA area. From our dataset, in cloud process case, analysis was impossible due to low abundance in gas-phase CHOCHO concentration (below detection limit).

4. Conclusions

In the present study, production rates and loss rates of CHOCHO were simulated using a 0-D box model constrained by high-quality gas, aerosol and meteorological measurements on board the NASA DC-8 during the KORUS-AQ mission, to elucidate the controllers of CHOCHO uptake to aerosols. High CHOCHO concentrations were observed over highly populated cities (i.e., Seoul) and industrial area, with peak concentration of 1.05 (2.10) ppb for 1 minute (10 seconds) average. Aromatics were the most important precursors of CHOCHO production (59 %), toluene being the highest contributor (41 %). We found the importance of the loss path to aerosol (69 %) followed by photolysis (19 %) and OH oxidation (12 %). Comparison of dilution-corrected P_{glySOA} to that of OA growth over the first 6 photochemical hours shows that glySOA contributes to ~20 % of SOA formation and oxalate yield from glySOA was estimated to be less than 10 % in Seoul. The $k_{eff,uptake}$ linearly increase with A_{surf} in Regime I ($A_{surf} < 4.9\times10^{-6}$ cm^2 cm^{-3}, $\gamma_{Gly,uptake} = 9.8\times10^{-3}$) but plateaus in Regime II ($A_{surf} > 4.9\times10^{-6}$ cm^2 cm^{-3}) which suggests the limitation in surface uptake approximation. This slower uptake under high aerosol loading condition can be attributed to the increased AN molality which likely induced high aerosol viscosity and thus, slow down CHOCHO mass transfer to aqueous phase. We also found light dependence of $k_{eff,uptake}$ suggesting the importance of photochemistry in ambient condition.

Finally, our work highlights the lacking knowledge to explain the CHOCHO solubility in real atmospheric circumstance. K_{H,eff_Gly} (~ 10^6 M atm^{-1}) derived from salting-in by AS and AN was not enough to describe CHOCHO loss by heterogeneous processes. This urges more attention to other various factors in CHOCHO solubility control in addition to the

https://doi.org/10.5194/acp-2021-672
Preprint. Discussion started: 31 August 2021


Atmospheric Chemistry and Physics Discussions

390 abundance of inorganic salts. Adding more constraints on these factors are important not only in SOA forming but also in air mass source tracking from satellite since CHOCHO is one of the two VOC proxies measured from space.

Data availability

DC8 data during KORUS-AQ are published at https://doi.org/10.5067/Suborbital/KORUSAQ/DATA01.

Author contribution

395 DK and KEM designed and executed the study and led the writing of the paper. DK, CC, SJ, KEM, SL, BAN, PCJ, DAD, JCS, JLJ, DRB, AW, AF, JPD, GSD, SEP, SRH, KU, LGH, DJT and JD provided observational data. RV and CJK contributed to aqueous phase mechanism model setups and data interpretation. BAN and PCJ ran E-AIM model. All coauthors contributed with feedback during the development and writing of the study.

Competing interests

400 The authors declare that they have no conflict of interest.

Acknowledgements

The authors thank all those who participated in the KORUS-AQ campaigns. We thank W.H. Brune for the HOx data, D. D. Montzka and A. J. Weinheimer for the NO_x, NO_y, and O_3 data, M. J. Kim, A. P. Teng, J. D. Crounse and P. O. Wennberg for HNO_3 data, B. E. Anderson group for the measurements from LARGE and J. Redemann, S. E. LeBlanc and M. Segal-
405 Rozenhaimer for the measurements from 4STAR. The PTR-MS instrument team, P. Eichler, L. Kaser, T. Mikoviny, M. Müller, is acknowledged for their support with field work and data processing. Ionicon Analytik is acknowledged for instrumental support.

Financial support

The Min group for CHOCHO measurements and analysis was supported by Technology Development Program to Solve
410 Climate Changes through the National Research Foundation of Korea (NRF) funded by the Ministry of Science, ICT (NRF 2019M1A2A2103953). The Jimenez group was supported by NASA 80NSSC18K0630 and NSF AGS-2027252. R. Volkamer was supported from the Department of Energy ASR program (award DE-SC0018221). A. Wisthaler group was supported from the Austrian Federal Ministry for Transport, Innovation and Technology (bmvit) through the Austrian Space Applications Programme (ASAP) of the Austrian Research Promotion Agency (FFG).

https://doi.org/10.5194/acp-2021-672
Preprint. Discussion started: 31 August 2021


Atmospheric Chemistry and Physics Discussions

415

References

Anderson, D. C., Nicely, J. M., Wolfe, G. M., Hanisco, T. F., Salawitch, R. J., Canty, T. P., Dickerson, R. R., Apel, E. C., Baidar, S., Bannan, T. J., Blake, N. J., Chen, D., Dix, B., Fernandez, R. P., Hall, S. R., Hornbrook, R. S., Huey, L. G., Josse, B., Jöckel, P., Kinnison, D. E., Koenig, T. K., LeBreton, M., Marécal, V., Morgenstern, O., Oman, L. D., Pan, L. L., Percival, C., Plummer, D., Revell, L. E., Rozanov, E., Saiz-Lopez, A., Stenke, A., Sudo, K., Tilmes, S., Ullmann, K., Volkamer, R., Weinheimer, A. J. and Zeng, G.: Formaldehyde in the Tropical Western Pacific: Chemical sources and sinks, convective transport, and representation in CAM-Chem and the CCMI models, J. Geophys. Res. D: Atmos., 122(20), 11201–11226, doi:10.1002/2016JD026121, 2017.

Bates, K. H. and Jacob, D. J.: A new model mechanism for atmospheric oxidation of isoprene: global effects on oxidants, nitrogen oxides, organic products, and secondary organic aerosol, Atmos. Chem. Phys., 19(14), 9613–9640, doi:10.5194/acp-19-9613-2019, 2019.

Blake, N. J., Blake, D. R., Simpson, I. J., Meinardi, S., Swanson, A. L., Lopez, J. P., Katzenstein, A. S., Barletta, B., Shirai, T., Atlas, Elliot, Sachse, G., Avery, M., Vay, S., Fuelberg, H. E., Kiley, C. M., Kita, K. and Rowland, F. S.: NMHCs and halocarbons in Asian continental outflow during the Transport and Chemical Evolution over the Pacific (TRACE-P) Field Campaign: Comparison With PEM-West B, J. Geophys. Res., 108(D20), doi:10.1029/2002jd003367, 2003.

Brock, C. A., Wagner, N. L., Anderson, B. E., Attwood, A. R., Beyersdorf, A., Campuzano-Jost, P., Carlton, A. G., Day, D. A., Diskin, G. S., Gordon, T. D., Jimenez, J. L., Lack, D. A., Liao, J., Markovic, M. Z., Middlebrook, A. M., Ng, N. L., Perring, A. E., Richardson, M. S., Schwarz, J. P., Washenfelder, R. A., Welti, A., Xu, L., Ziemba, L. D. and Murphy, D. M.: Aerosol optical properties in the southeastern United States in summer – Part 1: Hygroscopic growth, Atmos. Chem. Phys., 16(8), 4987–5007, doi:10.5194/acp-16-4987-2016, 2016.

Brune, W. H., Ren, X., Zhang, L., Mao, J., Miller, D. O., Anderson, B. E., Blake, D. R., Cohen, R. C., Diskin, G. S., Hall, S. R., Hanisco, T. F., Huey, L. G., Nault, B. A., Peischl, J., Pollack, I., Ryerson, T. B., Shingler, T., Sorooshian, A., Ullmann, K., Wisthaler, A. and Wooldridge, P. J.: Atmospheric oxidation in the presence of clouds during the Deep Convective Clouds and Chemistry (DC3) study, Atmos. Chem. Phys., 18(19), 14493–14510, doi:10.5194/acp-18-14493-2018, 2018.

Brune, W. H., Miller, D. O., Thames, A. B., Allen, H. M., Apel, E. C., Blake, D. R., Bui, T. P., Commane, R., Crounse, J. D., Daube, B. C., Diskin, G. S., DiGangi, J. P., Elkins, J. W., Hall, S. R., Hanisco, T. F., Hannun, R. A., Hintsa, E. J., Hornbrook, R. S., Kim, M. J., McKain, K., Moore, F. L., Neuman, J. A., Nicely, J. M., Peischl, J., Ryerson, T. B., St. Clair, J. M., Sweeney, C., Teng, A. P., Thompson, C., Ullmann, K., Veres, P. R., Wennberg, P. O. and Wolfe, G. M.: Exploring oxidation in the remote free troposphere: Insights from atmospheric tomography (ATom), J. Geophys. Res., 125(1), doi:10.1029/2019jd031685, 2020.

Canagaratna, M. R., Jayne, J. T., Jimenez, J. L., Allan, J. D., Alfarra, M. R., Zhang, Q., Onasch, T. B., Drewnick, F., Coe, H., Middlebrook, A., Delia, A., Williams, L. R., Trimborn, A. M., Northway, M. J., DeCarlo, P. F., Kolb, C. E., Davidovits, P. and Worsnop, D. R.: Chemical and microphysical characterization of ambient aerosols with the aerodyne aerosol mass spectrometer, Mass Spectrom. Rev., 26(2), 185–222, doi:10.1002/mas.20115, 2007.

Carlton, A. G., Turpin, B. J., Altieri, K. E., Seitzinger, S., Reff, A., Lim, H.-J. and Ervens, B.: Atmospheric oxalic acid and SOA production from glyoxal: Results of aqueous photooxidation experiments, Atmos. Environ., 41(35), 7588–7602, doi:10.1016/j.atmosenv.2007.05.035, 2007.

https://doi.org/10.5194/acp-2021-672
Preprint. Discussion started: 31 August 2021

Chan Miller, C., Jacob, D. J., González Abad, G. and Chance, K.: Hotspot of glyoxal over the Pearl River delta seen from the OMI satellite instrument: implications for emissions of aromatic hydrocarbons, Atmos. Chem. Phys., 16(7), 4631–4639, doi:10.5194/acp-16-4631-2016, 2016.

Chan Miller, C., Jacob, D. J., Marais, E. A., Yu, K., Travis, K. R., Kim, P. S., Fisher, J. A., Zhu, L., Wolfe, G. M., Hanisco, T. F., Keutsch, F. N., Kaiser, J., Min, K.-E., Brown, S. S., Washenfelder, R. A., González Abad, G. and Chance, K.: Glyoxal yield from isoprene oxidation and relation to formaldehyde: chemical mechanism, constraints from SENEX aircraft observations, and interpretation of OMI satellite data, Atmos. Chem. Phys., 17(14), 8725–8738, doi:10.5194/acp-17-8725-2017, 2017.

Clegg, S. L. and Brimblecombe, P.: Equilibrium partial pressures and mean activity and osmotic coefficients of 0-100% nitric acid as a function of temperature, J. Phys. Chem., 94(13), 5369–5380, doi:10.1021/j100376a038, 1990.

Clegg, S. L., Brimblecombe, P. and Wexler, A. S.: Thermodynamic Model of the System H^+–NH_4^+–Na^+–SO_4^{2-}–NO_3^-–Cl^-–H_2O at 298.15 K, J. Phys. Chem. A, 102(12), 2155–2171, doi:10.1021/jp973043j, 1998.

Corrigan, A. L., Hanley, S. W. and De Haan, D. O.: Uptake of glyoxal by organic and Inorganic aerosol, Environ. Sci. Technol., 42(12), 4428–4433, doi:10.1021/es7032394, 2008.

Crawford, J. H., Ahn, J.-Y., Al-Saadi, J., Chang, L., Emmons, L. K., Kim, J., Lee, G., Park, J.-H., Park, R. J., Woo, J. H., Song, C.-K., Hong, J.-H., Hong, Y.-D., Lefer, B. L., Lee, M., Lee, T., Kim, S., Min, K.-E., Yum, S. S., Shin, H. J., Kim, Y.-W., Choi, J.-S., Park, J.-S., Szykman, J. J., Long, R. W., Jordan, C. E., Simpson, I. J., Fried, A., Dibb, J. E., Cho, S. and Kim, Y. P.: The Korea–United States Air Quality (KORUS-AQ) field study, Elementa (Wash., DC), 9(1), doi:10.1525/elementa.2020.00163, 2021.

Crounse, J. D., McKinney, K. A., Kwan, A. J. and Wennberg, P. O.: Measurement of gas-phase hydroperoxides by chemical ionization mass spectrometry, Anal. Chem., 78(19), 6726–6732, doi:10.1021/ac0604235, 2006.

Curry, L. A., Tsui, W. G. and Faye McNeill, V.: Technical note: Updated parameterization of the reactive uptake of glyoxal and methylglyoxal by atmospheric aerosols and cloud droplets, Atmos. Chem. Phys., 18(13), 9823–9830, doi:10.5194/acp-18-9823-2018, 2018.

De Haan, D. O., Jansen, K., Rynaski, A. D., Sueme, W. R. P., Torkelson, A. K., Czer, E. T., Kim, A. K., Rafla, M. A., De Haan, A. C. and Tolbert, M. A.: Brown Carbon Production by Aqueous-Phase Interactions of Glyoxal and SO_2, Environ. Sci. Technol., 54(8), 4781–4789, doi:10.1021/acs.est.9b07852, 2020a.

De Haan, D. O., Hawkins, L. N., Jansen, K., Welsh, H. G., Pednekar, R., de Loera, A., Jimenez, N. G., Tolbert, M. A., Cazaunau, M., Gratien, A. and Others: Glyoxal's impact on dry ammonium salts: fast and reversible surface aerosol browning, Atmos. Chem. Phys., 20(16), 9581–9590, doi:10.5194/acp-20-9581-2020, 2020b.

DeCarlo, P. F., Kimmel, J. R., Trimborn, A., Northway, M. J., Jayne, J. T., Aiken, A. C., Gonin, M., Fuhrer, K., Horvath, T., Docherty, K. S., Worsnop, D. R. and Jimenez, J. L.: Field-deployable, high-resolution, time-of-flight aerosol mass spectrometer, Anal. Chem., 78(24), 8281–8289, doi:10.1021/ac061249n, 2006.

Dibb, J. E., Talbot, R. W. and Scheuer, E. M.: Composition and distribution of aerosols over the North Atlantic during the Subsonic Assessment Ozone and Nitrogen Oxide Experiment (SONEX), J. Geophys. Res., 105(D3), 3709–3717, doi:10.1029/1999jd900424, 2000.

Diskin, G. S., Podolske, J. R., Sachse, G. W. and Slate, T. A.: Open-path airborne tunable diode laser hygrometer, Proc. SPIE 4817, Diode Lasers and Applications in Atmospheric Sensing, doi: 10.1117/12.453736, 2002.

https://doi.org/10.5194/acp-2021-672
Preprint. Discussion started: 31 August 2021

Dunagan, S., Johnson, R., Zavaleta, J., Russell, P., Schmid, B., Flynn, C., Redemann, J., Shinozuka, Y., Livingston, J. and Segal-Rosenhaimer, M.: Spectrometer for sky-scanning sun-tracking atmospheric research (4STAR): Instrument technology, Remote Sens. (Basel), 5(8), 3872–3895, doi:10.3390/rs5083872, 2013.

Ervens, B. and Volkamer, R.: Glyoxal processing by aerosol multiphase chemistry: towards a kinetic modeling framework of secondary organic aerosol formation in aqueous particles, Atmos. Chem. Phys., 10(17), 8219–8244, doi:10.5194/acp-10-8219-2010, 2010.

Faloona, I. C., Tan, D., Lesher, R. L., Hazen, N. L., Frame, C. L., Simpas, J. B., Harder, H., Martinez, M., Di Carlo, P., Ren, X. and Brune, W. H.: A laser-induced fluorescence instrument for detecting tropospheric OH and HO_2: Characteristics and calibration, J. Atmos. Chem., 47(2), 139–167, doi:10.1023/b:joch.0000021036.53185.0e, 2004.

Feierabend, K. J., Zhu, L., Talukdar, R. K. and Burkholder, J. B.: Rate coefficients for the OH + HC(O)C(O)H (glyoxal) reaction between 210 and 390 K, J. Phys. Chem. A, 112(1), 73–82, doi:10.1021/jp0768571, 2008.

Feierabend, K. J., Flad, J. E., Brown, S. S. and Burkholder, J. B.: HCO quantum yields in the photolysis of HC(O)C(O)H (glyoxal) between 290 and 420 nm, J. Phys. Chem. A, 113(27), 7784–7794, doi:10.1021/jp9033003, 2009.

Friese, E. and Ebel, A.: Temperature dependent thermodynamic model of the system H^+-NH_4^+-Na^+-SO_4^{2-}-NO_3^--Cl^--H_2O, J. Phys. Chem. A, 114(43), 11595–11631, doi:10.1021/jp101041j, 2010.

Fu, T.-M., Jacob, D. J., Wittrock, F., Burrows, J. P., Vrekoussis, M. and Henze, D. K.: Global budgets of atmospheric glyoxal and methylglyoxal, and implications for formation of secondary organic aerosols, J. Geophys. Res., 113(D15), doi:10.1029/2007jd009505, 2008.

Galloway, M. M., Chhabra, P. S., Chan, A. W. H., Surratt, J. D., Flagan, R. C., Seinfeld, J. H. and Keutsch, F. N.: Glyoxal uptake on ammonium sulphate seed aerosol: reaction products and reversibility of uptake under dark and irradiated conditions, Atmos. Chem. Phys., 9(10), 3331–3345, doi:10.5194/acp-9-3331-2009, 2009.

Galloway, M. M., Loza, C. L., Chhabra, P. S., Chan, A. W. H., Yee, L. D., Seinfeld, J. H. and Keutsch, F. N.: Analysis of photochemical and dark glyoxal uptake: Implications for SOA formation, Geophys. Res. Lett., 38(17), doi:10.1029/2011gl048514, 2011.

Gen, M., Huang, D. D. and Chan, C. K.: Reactive Uptake of Glyoxal by Ammonium-Containing Salt Particles as a Function of Relative Humidity, Environ. Sci. Technol., 52(12), 6903–6911, doi:10.1021/acs.est.8b00606, 2018.

Gomez, M. E., Lin, Y., Guo, S. and Zhang, R.: Heterogeneous chemistry of glyoxal on acidic solutions. An oligomerization pathway for secondary organic aerosol formation, J. Phys. Chem. A, 119(19), 4457–4463, doi:10.1021/jp509916r, 2015.

Gorkowski, K., Donahue, N. M. and Sullivan, R. C.: Aerosol Optical Tweezers Constrain the Morphology Evolution of Liquid-Liquid Phase-Separated Atmospheric Particles, Chem, 6(1), 204–220, doi:10.1016/j.chempr.2019.10.018, 2020.

Haskins, J. D., Lopez-Hilfiker, F. D., Lee, B. H., Shah, V., Wolfe, G. M., DiGangi, J., Fibiger, D., McDuffie, E. E., Veres, P., Schroder, J. C., Campuzano-Jost, P., Day, D. A., Jimenez, J. L., Weinheimer, A., Sparks, T., Cohen, R. C., Campos, T., Sullivan, A., Guo, H., Weber, R., Dibb, J., Greene, J., Fiddler, M., Bililign, S., Jaeglé, L., Brown, S. S. and Thornton, J. A.: Anthropogenic control over wintertime oxidation of atmospheric pollutants, Geophys. Res. Lett., 46(24), 14826–14835, doi:10.1029/2019GL085498, 2019.

Hastings, W. P., Koehler, C. A., Bailey, E. L. and De Haan, D. O.: Secondary organic aerosol formation by glyoxal hydration and oligomer formation: humidity effects and equilibrium shifts during analysis, Environ. Sci. Technol., 39(22), 8728–8735, doi:10.1021/es050446l, 2005.

https://doi.org/10.5194/acp-2021-672
Preprint. Discussion started: 31 August 2021

Atmospheric Chemistry and Physics Discussions

Herrmann, H., Hoffmann, D., Schaefer, T., Bräuer, P. and Tilgner, A.: Tropospheric aqueous-phase free-radical chemistry: radical sources, spectra, reaction kinetics and prediction tools, ChemPhysChem, 11(18), 3796–3822, doi:10.1002/cphc.201000533, 2010.

Hu, J., Wang, P., Ying, Q., Zhang, H., Chen, J., Ge, X., Li, X., Jiang, J., Wang, S., Zhang, J., Zhao, Y. and Zhang, Y.: Modeling biogenic and anthropogenic secondary organic aerosol in China, Atmos. Chem. Phys., 17(1), 77–92, doi:10.5194/acp-17-77-2017, 2017.

Huey, L. G., Tanner, D. J., Slusher, D. L., Dibb, J. E., Arimoto, R., Chen, G., Davis, D., Buhr, M. P., Nowak, J. B., Mauldin, R. L., Eisele, F. L. and Kosciuch, E.: CIMS measurements of HNO_3 and SO_2 at the South Pole during ISCAT 2000, Atmos. Environ., 38(32), 5411–5421, doi:10.1016/j.atmosenv.2004.04.037, 2004.

Ip, H. S. S., Huang, X. H. H. and Yu, J. Z.: Effective Henry's law constants of glyoxal, glyoxylic acid, and glycolic acid, Geophys. Res. Lett., 36(1), doi:10.1029/2008gl036212, 2009.

Jang, M. and Kamens, R. M.: Atmospheric secondary aerosol formation by heterogeneous reactions of aldehydes in the presence of a sulfuric acid aerosol catalyst, Environ. Sci. Technol., 35(24), 4758–4766, doi:10.1021/es010790s, 2001.

Jenkin, M. E., Young, J. C. and Rickard, A. R.: The MCM v3.3.1 degradation scheme for isoprene, Atmos. Chem. Phys., 15(20), 11433–11459, doi:10.5194/acp-15-11433-2015, 2015.

Kaiser, J., Wolfe, G. M., Min, K. E., Brown, S. S., Miller, C. C., Jacob, D. J., DeGouw, J. A., Graus, M., Hanisco, T. F., Holloway, J. and Others: Reassessing the ratio of glyoxal to formaldehyde as an indicator of hydrocarbon precursor speciation, Atmos. Chem. Phys., 15(13), 7571–7583, doi:10.5194/acp-15-7571-2015, 2015.

Kaiser, J., Skog, K. M., Baumann, K., Bertman, S. B., Brown, S. B., Brune, W. H., Crounse, J. D., de Gouw, J. A., Edgerton, E. S., Feiner, P. A., Goldstein, A. H., Koss, A., Misztal, P. K., Nguyen, T. B., Olson, K. F., St. Clair, J. M., Teng, A. P., Toma, S., Wennberg, P. O., Wild, R. J., Zhang, L. and Keutsch, F. N.: Speciation of OH reactivity above the canopy of an isoprene-dominated forest, Atmos. Chem. Phys., 16(14), 9349–9359, doi:10.5194/acp-16-9349-2016, 2016.

Kampf, C. J., Waxman, E. M., Slowik, J. G., Dommen, J., Pfaffenberger, L., Praplan, A. P., Prévôt, A. S. H., Baltensperger, U., Hoffmann, T. and Volkamer, R.: Effective Henry's law partitioning and the salting constant of glyoxal in aerosols containing sulfate, Environ. Sci. Technol., 47(9), 4236–4244, doi:10.1021/es400083d, 2013.

Klaning, U. K., Sehested, K. and Holcman, J.: Standard Gibbs energy of formation of the hydroxyl radical in aqueous solution. Rate constants for the reaction $ClO_2^- + O_3 \leftrightarrow O_3^- + ClO_2$, J. Phys. Chem., 89(5), 760–763, doi:10.1021/j100251a008, 1985.

Kleinman, L. I., Daum, P. H., Lee, Y.-N., Nunnermacker, L. J., Springston, S. R., Weinstein-Lloyd, J., Hyde, P., Doskey, P., Rudolph, J., Fast, J. and Berkowitz, C.: Photochemical age determinations in the Phoenix metropolitan area, J. Geophys. Res., 108(D3), doi:10.1029/2002jd002621, 2003.

Knote, C., Hodzic, A., Jimenez, J. L., Volkamer, R., Orlando, J. J., Baidar, S., Brioude, J., Fast, J., Gentner, D. R., Goldstein, A. H., Hayes, P. L., Knighton, W. B., Oetjen, H., Setyan, A., Stark, H., Thalman, R., Tyndall, G., Washenfelder, R., Waxman, E. and Zhang, Q.: Simulation of semi-explicit mechanisms of SOA formation from glyoxal in aerosol in a 3-D model, Atmos. Chem. Phys., 14(12), 6213–6239, doi:10.5194/acp-14-6213-2014, 2014.

Kraus, S.: DOASIS: a framework design for DOAS, Shaker Verlag, Aachen, Germany., 2006.

Kroll, J. H., Ng, N. L., Murphy, S. M., Varutbangkul, V., Flagan, R. C. and Seinfeld, J. H.: Chamber studies of secondary organic aerosol growth by reactive uptake of simple carbonyl compounds, J. Geophys. Res., 110(D23), doi:10.1029/2005jd006004, 2005.

https://doi.org/10.5194/acp-2021-672
Preprint. Discussion started: 31 August 2021


Atmospheric Chemistry and Physics Discussions

Lee, A. K. Y., Herckes, P., Leaitch, W. R., Macdonald, A. M. and Abbatt, J. P. D.: Aqueous OH oxidation of ambient organic aerosol and cloud water organics: Formation of highly oxidized products, Geophys. Res. Lett., 38(11), doi:10.1029/2011gl047439, 2011.

Li, J., Mao, J., Min, K.-E., Washenfelder, R. A., Brown, S. S., Kaiser, J., Keutsch, F. N., Volkamer, R., Wolfe, G. M., Hanisco, T. F., Pollack, I. B., Ryerson, T. B., Graus, M., Gilman, J. B., Lerner, B. M., Warneke, C., de Gouw, J. A., Middlebrook, A. M., Liao, J., Welti, A., Henderson, B. H., McNeill, V. F., Hall, S. R., Ullmann, K., Donner, L. J., Paulot, F. and Horowitz, L. W.: Observational constraints on glyoxal production from isoprene oxidation and its contribution to organic aerosol over the Southeast United States, J. Geophys. Res. D: Atmos., 121(16), 9849–9861, doi:10.1002/2016JD025331, 2016.

Liggio, J., Li, S.-M. and McLaren, R.: Heterogeneous Reactions of Glyoxal on Particulate Matter: Identification of Acetals and Sulfate Esters, Environ. Sci. Technol., 39(6), 1532–1541, doi:10.1021/es048375y, 2005a.

Liggio, J., Li, S.-M. and McLaren, R.: Reactive uptake of glyoxal by particulate matter, J. Geophys. Res., 110(D10), doi:10.1029/2004jd005113, 2005b.

Lim, Y. B., Tan, Y. and Turpin, B. J.: Chemical insights, explicit chemistry, and yields of secondary organic aerosol from OH radical oxidation of methylglyoxal and glyoxal in the aqueous phase, Atmos. Chem. Phys., 13(17), 8651–8667, doi:10.5194/acp-13-8651-2013, 2013.

Lim, Y. B., Kim, H., Kim, J. Y. and Turpin, B. J.: Photochemical organonitrate formation in wet aerosols, Atmos. Chem. Phys., 16(19), 12631–12647, doi:10.5194/acp-16-12631-2016, 2016.

Ling, Z., Xie, Q., Shao, M., Wang, Z., Wang, T., Guo, H. and Wang, X.: Formation and sink of glyoxal and methylglyoxal in a polluted subtropical environment: observation-based photochemical analysis and impact evaluation, Atmos. Chem. Phys., 20(19), 11451–11467, doi:10.5194/acp-20-11451-2020, 2020.

Liu, J., Shen, J., Cheng, Z., Wang, P., Ying, Q., Zhao, Q., Zhang, Y., Zhao, Y. and Fu, Q.: Source apportionment and regional transport of anthropogenic secondary organic aerosol during winter pollution periods in the Yangtze River Delta, China, Sci. Total Environ., 710, 135620, doi:10.1016/j.scitotenv.2019.135620, 2020.

Loeffler, K. W., Koehler, C. A., Paul, N. M. and De Haan, D. O.: Oligomer formation in evaporating aqueous glyoxal and methyl glyoxal solutions, Environ. Sci. Technol., 40(20), 6318–6323, doi:10.1021/es060810w, 2006.

MacDonald, S. M., Oetjen, H., Mahajan, A. S., Whalley, L. K., Edwards, P. M., Heard, D. E., Jones, C. E. and Plane, J. M. C.: DOAS measurements of formaldehyde and glyoxal above a south-east Asian tropical rainforest, Atmos. Chem. Phys., 12(13), 5949–5962, doi:10.5194/acp-12-5949-2012, 2012.

Marrero-Ortiz, W., Hu, M., Du, Z., Ji, Y., Wang, Y., Guo, S., Lin, Y., Gomez-Hermandez, M., Peng, J., Li, Y., Secrest, J., Zamora, M. L., Wang, Y., An, T. and Zhang, R.: Formation and Optical Properties of Brown Carbon from Small α-Dicarbonyls and Amines, Environ. Sci. Technol., 53(1), 117–126, doi:10.1021/acs.est.8b03995, 2019.

Marvin, M. R., Wolfe, G. M., Salawitch, R. J., Canty, T. P., Roberts, S. J., Travis, K. R., Aikin, K. C., de Gouw, J. A., Graus, M., Hanisco, T. F., Holloway, J. S., Hübler, G., Kaiser, J., Keutsch, F. N., Peischl, J., Pollack, I. B., Roberts, J. M., Ryerson, T. B., Veres, P. R. and Warneke, C.: Impact of evolving isoprene mechanisms on simulated formaldehyde: An inter-comparison supported by in situ observations from SENEX, Atmos. Environ., 164, 325–336, doi:10.1016/j.atmosenv.2017.05.049, 2017.

Massucci, M., Clegg, S. L. and Brimblecombe, P.: Equilibrium Partial Pressures, Thermodynamic Properties of Aqueous and Solid Phases, and Cl2 Production from Aqueous HCl and HNO_3 and Their Mixtures, J. Phys. Chem. A, 103(21), 4209–4226, doi:10.1021/jp9847179, 1999.

https://doi.org/10.5194/acp-2021-672
Preprint. Discussion started: 31 August 2021


Atmospheric Chemistry and Physics Discussions

McNaughton, C. S., Clarke, A. D., Howell, S. G., Pinkerton, M., Anderson, B., Thornhill, L., Hudgins, C., Winstead, E., Dibb, J. E., Scheuer, E. and Maring, H.: Results from the DC-8 Inlet Characterization Experiment (DICE): Airborne Versus Surface Sampling of Mineral Dust and Sea Salt Aerosols, Aerosol Sci. Technol., 41(2), 136–159, doi:10.1080/02786820601118406, 2007.

Min, K.-E., Washenfelder, R. A., Dubé, W. P., Langford, A. O., Edwards, P. M., Zarzana, K. J., Stutz, J., Lu, K., Rohrer, F., Zhang, Y. and Brown, S. S.: A broadband cavity enhanced absorption spectrometer for aircraft measurements of glyoxal, methylglyoxal, nitrous acid, nitrogen dioxide, and water vapor, Atmos. Meas. Tech., 9(2), 423–440, doi:10.5194/amt-9-423-2016, 2016.

Mollner, A. K., Valluvadasan, S., Feng, L., Sprague, M. K., Okumura, M., Milligan, D. B., Bloss, W. J., Sander, S. P., Martien, P. T., Harley, R. A., McCoy, A. B. and Carter, W. P. L.: Rate of gas phase association of hydroxyl radical and nitrogen dioxide, Science, 330(6004), 646–649, doi:10.1126/science.1193030, 2010.

Monge, M. E., Rosenørn, T., Favez, O., Müller, M., Adler, G., Abo Riziq, A., Rudich, Y., Herrmann, H., George, C. and D'Anna, B.: Alternative pathway for atmospheric particles growth, Proc. Natl. Acad. Sci. U. S. A., 109(18), 6840–6844, doi:10.1073/pnas.1120593109, 2012.

Müller, M., Mikoviny, T., Feil, S., Haidacher, S., Hanel, G., Hartungen, E., Jordan, A., Märk, L., Mutschlechner, P., Schottkowsky, R., Sulzer, P., Crawford, J. H. and Wisthaler, A.: A compact PTR-ToF-MS instrument for airborne measurements of volatile organic compounds at high spatiotemporal resolution, Atmos. Meas. Tech., 7(11), 3763–3772, doi:10.5194/amt-7-3763-2014, 2014.

Nault, B. A., Campuzano-Jost, P., Day, D. A., Schroder, J. C., Anderson, B., Beyersdorf, A. J., Blake, D. R., Brune, W. H., Choi, Y., Corr, C. A., de Gouw, J. A., Dibb, J., DiGangi, J. P., Diskin, G. S., Fried, A., Huey, L. G., Kim, M. J., Knote, C. J., Lamb, K. D., Lee, T., Park, T., Pusede, S. E., Scheuer, E., Thornhill, K. L., Woo, J.-H. and Jimenez, J. L.: Secondary organic aerosol production from local emissions dominates the organic aerosol budget over Seoul, South Korea, during KORUS-AQ, Atmos. Chem. Phys., 18(24), 17769–17800, doi:10.5194/acp-18-17769-2018, 2018.

Nishino, N., Arey, J. and Atkinson, R.: Formation yields of glyoxal and methylglyoxal from the gas-phase OH radical-initiated reactions of toluene, xylenes, and trimethylbenzenes as a function of NO_2 concentration, J. Phys. Chem. A, 114(37), 10140–10147, doi:10.1021/jp105112h, 2010.

Olson, J. R., Crawford, J. H., Chen, G., Brune, W. H., Faloona, I. C., Tan, D., Harder, H. and Martinez, M.: A reevaluation of airborne HOxobservations from NASA field campaigns, J. Geophys. Res., 111(D10), doi:10.1029/2005jd006617, 2006.

Ortiz-Montalvo, D. L., Häkkinen, S. A. K., Schwier, A. N., Lim, Y. B., McNeill, V. F. and Turpin, B. J.: Ammonium addition (and aerosol pH) has a dramatic impact on the volatility and yield of glyoxal secondary organic aerosol, Environ. Sci. Technol., 48(1), 255–262, doi:10.1021/es4035667, 2014.

Paulson, S. E., Gallimore, P. J., Kuang, X. M., Chen, J. R., Kalberer, M. and Gonzalez, D. H.: A light-driven burst of hydroxyl radicals dominates oxidation chemistry in newly activated cloud droplets, Sci Adv, 5(5), eaav7689, doi:10.1126/sciadv.aav7689, 2019.

Peterson, D. A., Hyer, E. J., Han, S.-O., Crawford, J. H., Park, R. J., Holz, R., Kuehn, R. E., Eloranta, E., Knote, C., Jordan, C. E. and Lefer, B. L.: Meteorology influencing springtime air quality, pollution transport, and visibility in Korea, Elementa (Wash., DC), 7(1), 57, doi:10.1525/elementa.395, 2019.

Powelson, M. H., Espelien, B. M., Hawkins, L. N., Galloway, M. M. and De Haan, D. O.: Brown carbon formation by aqueous-phase carbonyl compound reactions with amines and ammonium sulfate, Environ. Sci. Technol., 48(2), 985–993, doi:10.1021/es4038325, 2014.

https://doi.org/10.5194/acp-2021-672
Preprint. Discussion started: 31 August 2021


Atmospheric Chemistry and Physics Discussions

Qin, Y., Ye, J., Ohno, P. E., Lei, Y., Wang, J., Liu, P., Thomson, R. J. and Martin, S. T.: Synergistic Uptake by Acidic Sulfate Particles of Gaseous Mixtures of Glyoxal and Pinanediol, Environ. Sci. Technol., 54(19), 11762–11770, doi:10.1021/acs.est.0c02062, 2020.

Qiu, X., Wang, S., Ying, Q., Duan, L., Xing, J., Cao, J., Wu, D., Li, X., Chengzhi, X., Yan, X., Liu, C. and Hao, J.: Importance of Wintertime Anthropogenic Glyoxal and Methylglyoxal Emissions in Beijing and Implications for Secondary Organic Aerosol Formation in Megacities, Environ. Sci. Technol., 54(19), 11809–11817, doi:10.1021/acs.est.0c02822, 2020.

Richter, D., Weibring, P., Walega, J. G., Fried, A., Spuler, S. M. and Taubman, M. S.: Compact highly sensitive multi-species airborne mid-IR spectrometer, Appl. Phys. B, 119(1), 119–131, doi:10.1007/s00340-015-6038-8, 2015.

Rickards, A. M. J., Miles, R. E. H., Davies, J. F., Marshall, F. H. and Reid, J. P.: Measurements of the sensitivity of aerosol hygroscopicity and the κ parameter to the O/C ratio, J. Phys. Chem. A, 117(51), 14120–14131, doi:10.1021/jp407991n, 2013.

Rossignol, S., Aregahegn, K. Z., Tinel, L., Fine, L., Nozière, B. and George, C.: Glyoxal induced atmospheric photosensitized chemistry leading to organic aerosol growth, Environ. Sci. Technol., 48(6), 3218–3227, doi:10.1021/es405581g, 2014.

Sachse, G. W., Hill, G. F., Wade, L. O. and Perry, M. G.: Fast-response, high-precision carbon monoxide sensor using a tunable diode laser absorption technique, J. Geophys. Res., 92(D2), 2071, doi:10.1029/jd092id02p02071, 1987.

Sareen, N., Waxman, E. M., Turpin, B. J., Volkamer, R. and Carlton, A. G.: Potential of aerosol liquid water to facilitate organic aerosol formation: Assessing knowledge gaps about precursors and partitioning, Environ. Sci. Technol., 51(6), 3327–3335, doi:10.1021/acs.est.6b04540, 2017.

Schroeder, J. R., Crawford, J. H., Ahn, J.-Y., Chang, L., Fried, A., Walega, J., Weinheimer, A., Montzka, D. D., Hall, S. R., Ullmann, K., Wisthaler, A., Mikoviny, T., Chen, G., Blake, D. R., Blake, N. J., Hughes, S. C., Meinardi, S., Diskin, G., Digangi, J. P., Choi, Y., Pusede, S. E., Huey, G. L., Tanner, D. J., Kim, M. and Wennberg, P.: Observation-based modeling of ozone chemistry in the Seoul metropolitan area during the Korea-United States Air Quality Study (KORUS-AQ), Elementa (Wash., DC), 8(1), 3, doi:10.1525/elementa.400, 2020.

Seinfeld, J. H. and Pandis, S. N.: Atmospheric Chemistry and Physics: From Air Pollution to Climate Change, 3rd Edition, Wiley., 2016.

Shen, H., Chen, Z., Li, H., Qian, X., Qin, X. and Shi, W.: Gas-Particle Partitioning of Carbonyl Compounds in the Ambient Atmosphere, Environ. Sci. Technol., 52(19), 10997–11006, doi:10.1021/acs.est.8b01882, 2018.

Shetter, R. E. and Müller, M.: Photolysis frequency measurements using actinic flux spectroradiometry during the PEM-Tropics mission: Instrumentation description and some results, J. Geophys. Res., 104(D5), 5647–5661, doi:10.1029/98jd01381, 1999.

Shi, Q., Zhang, W., Ji, Y., Wang, J., Qin, D., Chen, J., Gao, Y., Li, G. and An, T.: Enhanced uptake of glyoxal at the acidic nanoparticle interface: implications for secondary organic aerosol formation, Environ. Sci.: Nano, 7(4), 1126–1135, doi:10.1039/D0EN00016G, 2020.

Simpson, I. J., Blake, D. R., Blake, N. J., Meinardi, S., Barletta, B., Hughes, S. C., Fleming, L. T., Crawford, J. H., Diskin, G. S., Emmons, L. K., Fried, A., Guo, H., Peterson, D. A., Wisthaler, A., Woo, J.-H., Barré, J., Gaubert, B., Kim, J., Kim, M. J., Kim, Y., Knote, C., Mikoviny, T., Pusede, S. E., Schroeder, J. R., Wang, Y., Wennberg, P. O. and Zeng, L.: Characterization, sources and reactivity of volatile organic compounds (VOCs) in Seoul and surrounding regions during KORUS-AQ, Elementa (Wash., DC), 8(1), 37, doi:10.1525/elementa.434, 2020.

Song, M., Ham, S., Andrews, R. J., You, Y. and Bertram, A. K.: Liquid–liquid phase separation in organic particles containing one and two organic species: importance of the average O : C, Atmos. Chem. Phys., 18(16), 12075–12084, doi:10.5194/acp-18-12075-2018, 2018.

Song, M., Maclean, A. M., Huang, Y., Smith, N. R., Blair, S. L., Laskin, J., Laskin, A., DeRieux, W.-S. W., Li, Y., Shiraiwa, M., Nizkorodov, S. A. and Bertram, A. K.: Liquid–liquid phase separation and viscosity within secondary organic aerosol generated from diesel fuel vapors, Atmos. Chem. Phys., 19(19), 12515–12529, doi:10.5194/acp-19-12515-2019, 2019.

Souri, A. H., Nowlan, C. R., Wolfe, G. M., Lamsal, L. N., Chan Miller, C. E., Abad, G. G., Janz, S. J., Fried, A., Blake, D. R., Weinheimer, A. J., Diskin, G. S., Liu, X. and Chance, K.: Revisiting the effectiveness of HCHO/NO_2 ratios for inferring ozone sensitivity to its precursors using high resolution airborne remote sensing observations in a high ozone episode during the KORUS-AQ campaign, Atmos. Environ., 224, 117341, doi:10.1016/j.atmosenv.2020.117341, 2020.

Stadtler, S., Kühn, T., Schröder, S., Taraborrelli, D., Schultz, M. G. and Kokkola, H.: Isoprene-derived secondary organic aerosol in the global aerosol–chemistry–climate model ECHAM6.3.0–HAM2.3–MOZ1.0, Geosci. Model Dev., 11(8), 3235–3260, doi:10.5194/gmd-11-3235-2018, 2018.

Sumner, A. J., Woo, J. L. and McNeill, V. F.: Model analysis of secondary organic aerosol formation by glyoxal in laboratory studies: the case for photoenhanced chemistry, Environ. Sci. Technol., 48(20), 11919–11925, doi:10.1021/es502020j, 2014.

Tan, Y., Perri, M. J., Seitzinger, S. P. and Turpin, B. J.: Effects of precursor concentration and acidic sulfate in aqueous glyoxal-OH radical oxidation and implications for secondary organic aerosol, Environ. Sci. Technol., 43(21), 8105–8112, doi:10.1021/es901742f, 2009.

Tang, M. J., Shiraiwa, M., Pöschl, U., Cox, R. A. and Kalberer, M.: Compilation and evaluation of gas phase diffusion coefficients of reactive trace gases in the atmosphere: Volume 2. Diffusivities of organic compounds, pressure-normalised mean free paths, and average Knudsen numbers for gas uptake calculations, Atmos. Chem. Phys., 15(10), 5585–5598, doi:10.5194/acp-15-5585-2015, 2015.

Tong, H., Arangio, A. M., Lakey, P. S. J., Berkemeier, T., Liu, F., Kampf, C. J., Brune, W. H., Pöschl, U. and Shiraiwa, M.: Hydroxyl radicals from secondary organic aerosol decomposition in water, Atmos. Chem. Phys., 16(3), 1761–1771, doi:10.5194/acp-16-1761-2016, 2016.

Volkamer, R., Platt, U. and Wirtz, K.: Primary and Secondary Glyoxal Formation from Aromatics: Experimental Evidence for the Bicycloalkyl−Radical Pathway from Benzene, Toluene, and p-Xylene, J. Phys. Chem. A, 105(33), 7865–7874, doi:10.1021/jp010152w, 2001.

Volkamer, R., San Martini, F., Molina, L. T., Salcedo, D., Jimenez, J. L. and Molina, M. J.: A missing sink for gas-phase glyoxal in Mexico City: Formation of secondary organic aerosol, Geophys. Res. Lett., 34(19), doi:10.1029/2007gl030752, 2007.

Volkamer, R., Ziemann, P. J. and Molina, M. J.: Secondary Organic Aerosol Formation from Acetylene (C_2H_2): seed effect on SOA yields due to organic photochemistry in the aerosol aqueous phase, Atmos. Chem. Phys., 9(6), 1907–1928, doi:10.5194/acp-9-1907-2009, 2009.

Walega, J. G., Dye, J. E., Grahek, F. E. and Ridley, B. K.: Compact measurement system for the simultaneous determination of NO, NO_2, NO_y, and O_3 using a small aircraft, in Measurement of Atmospheric Gases, vol. 1433, pp. 232–241, International Society for Optics and Photonics., 1991.

Washenfelder, R. A., Young, C. J., Brown, S. S., Angevine, W. M., E. L. Atlas, Blake, D. R., Bon, D. M., Cubison, M. J., de Gouw, J. A., Dusanter, S., Flynn, J., Gilman, J. B., Graus, M., Griffith, S., Grossberg, N., Hayes, P. L., Jimenez, J. L.,

https://doi.org/10.5194/acp-2021-672
Preprint. Discussion started: 31 August 2021

Atmospheric Chemistry and Physics Discussions

Kuster, W. C., Lefer, B. L., Pollack, I. B., Ryerson, T. B., Stark, H., Stevens, P. S. and Trainer, M. K.: The glyoxal budget and its contribution to organic aerosol for Los Angeles, California, during CalNex 2010, J. Geophys. Res., 116(D21), doi:10.1029/2011jd016314, 2011.

Waxman, E. M., Dzepina, K., Ervens, B., Lee-Taylor, J., Aumont, B., Jimenez, J. L., Madronich, S. and Volkamer, R.: Secondary organic aerosol formation from semi- and intermediate-volatility organic compounds and glyoxal: Relevance of O/C as a tracer for aqueous multiphase chemistry, Geophys. Res. Lett., 40(5), 978–982, doi:10.1002/grl.50203, 2013.

Waxman, E. M., Elm, J., Kurtén, T., Mikkelsen, K. V., Ziemann, P. J. and Volkamer, R.: Glyoxal and Methylglyoxal Setschenow Salting Constants in Sulfate, Nitrate, and Chloride Solutions: Measurements and Gibbs Energies, Environ. Sci. Technol., 49(19), 11500–11508, doi:10.1021/acs.est.5b02782, 2015.

Wexler, A. S.: Atmospheric aerosol models for systems including the ions H^+, NH_4^+, Na^+, SO_4^{2-}, NO_3^-, Cl^-, Br^-, and H_2O, J. Geophys. Res., 107(D14), doi:10.1029/2001jd000451, 2002.

Whipple, E. B.: Structure of glyoxal in water, J. Am. Chem. Soc., 92(24), 7183–7186, doi:10.1021/ja00727a027, 1970.

Wisthaler, A.: Organic trace gas measurements by PTR-MS during INDOEX 1999, J. Geophys. Res., 107(D19), doi:10.1029/2001jd000576, 2002.

Wolfe, G. M., Marvin, M. R., Roberts, S. J., Travis, K. R. and Liao, J.: The Framework for 0-D Atmospheric Modeling (F0AM) v3.1, Geosci. Model Dev., 9(9), 3309–3319, doi:10.5194/gmd-9-3309-2016, 2016.

Xu, Y., Chen, Y., Gao, J., Zhu, S., Ying, Q., Hu, J., Wang, P., Feng, L., Kang, H. and Wang, D.: Contribution of biogenic sources to secondary organic aerosol in the summertime in Shaanxi, China, Chemosphere, 254, 126815, doi:10.1016/j.chemosphere.2020.126815, 2020.

Yu, G., Bayer, A. R., Galloway, M. M., Korshavn, K. J., Fry, C. G. and Keutsch, F. N.: Glyoxal in aqueous ammonium sulfate solutions: products, kinetics and hydration effects, Environ. Sci. Technol., 45(15), 6336–6342, doi:10.1021/es200989n, 2011.

Zarzana, K. J., Min, K.-E., Washenfelder, R. A., Kaiser, J., Krawiec-Thayer, M., Peischl, J., Neuman, J. A., Nowak, J. B., Wagner, N. L., Dubè, W. P., St Clair, J. M., Wolfe, G. M., Hanisco, T. F., Keutsch, F. N., Ryerson, T. B. and Brown, S. S.: Emissions of Glyoxal and Other Carbonyl Compounds from Agricultural Biomass Burning Plumes Sampled by Aircraft, Environ. Sci. Technol., 51(20), 11761–11770, doi:10.1021/acs.est.7b03517, 2017.

Zarzana, K. J., Selimovic, V., Koss, A. R., Sekimoto, K., Coggon, M. M., Yuan, B., Dubé, W. P., Yokelson, R. J., Warneke, C., de Gouw, J. A., Roberts, J. M. and Brown, S. S.: Primary emissions of glyoxal and methylglyoxal from laboratory measurements of open biomass burning, Atmos. Chem. Phys., 18(20), 15451–15470, doi:10.5194/acp-18-15451-2018, 2018.

Zhou, X. and Mopper, K.: Apparent partition coefficients of 15 carbonyl compounds between air and seawater and between air and freshwater; implications for air-sea exchange, Environ. Sci. Technol., 24(12), 1864–1869, doi:10.1021/es00082a013, 1990.

https://doi.org/10.5194/acp-2021-672
Preprint. Discussion started: 31 August 2021

Atmospheric Chemistry and Physics Discussions

Table 1. Measurements from DC-8 used in this study.

Species	Instrument Name/Technique	Time resolution	Reference
NO, NO_2, NO_y[a], O_3	NCAR 4-Channel Chemiluminescence Instrument	1 s	Walega et al. (1991)
SO_2	GT-CIMS[b]	1 s	Huey et al. (2004)
HNO_3	CIT-CIMS[c]	1s	Crounse et al. (2006)
OH, HO_2, OH reactivity	ATHOS[d]	20 s	Faloona et al. (2004)
CO, CH_4	DACOM[e]	1 s	Sachse et al. (1987)
VOCs	WAS[f]	1-5 min	Blake et al. (2003), Simpson et al. (2020)
VOCs	PTR-ToF-MS[g]	1 s	Wisthaler (2002), Müller et al. (2014)
HCHO, C_2H_6	CAMS[h]	1 s	Richter et al. (2015)
CHOCHO	CAESAR[i]	10 s	Min et al. (2016)
Relative humidity	DLH[j]	1 s	Diskin et al. (2002)
Aerosol chemical composition (OA, SO_4, NO_3, NH_4)	HR-ToF-AMS[k]	1 s	DeCarlo et al. (2006), Canagaratna et al. (2007), Nault et al. (2018)
Oxalate	SAGA[l] filter	5-10 min	Dibb et al. (2000), McNaughton et al. (2007)
Aerosol size distribution	LARGE[m] SMPS[n] and LAS[o]	63 s (SMPS) / 1 s (LAS)	
Actinic Flux	CAFS[p]	1 s	Shetter and Müller (1999)
O_3 column density	4STAR[q]	1 s	Dunagan et al. (2013)

[a]Total reactive nitrogen, [b]Georgia Institute of Technology - Chemical Ionization Mass Spectrometer, [c]California Institute of Technology - Chemical Ionization Mass Spectrometer, [d]Airborne Tropospheric Hydrogen Oxides Sensor, [e]Differential Absorption Carbon monOxide Measurements, [f]Whole Air Sampler, [g]Proton Transfer Reaction Time-of-Flight Mass Spectrometer, [h]Compact Atmospheric Multi-Species Spectrometer, [i]CAvity Enhanced Absorption Spectrometer for Atmospheric Research, [j]Diode Laser Hygrometer, [k]High Resolution Time-of-Flight Aerosol Mass Spectrometer, [l]Soluble Acidic Gases and Aerosols, [m]Langley Aerosol Research Group Experiment, [n]Scanning Mobility Particle Sizer (SMPS, TSI model 3936), [o]Laser Aerosol Spectrometer (LAS, TSI model 3340), [p]CCD Actinic Flux Spectrometers, [q]Spectrometers for Sky-Scanning, Sun-Tracking Atmospheric Research.

https://doi.org/10.5194/acp-2021-672
Preprint. Discussion started: 31 August 2021

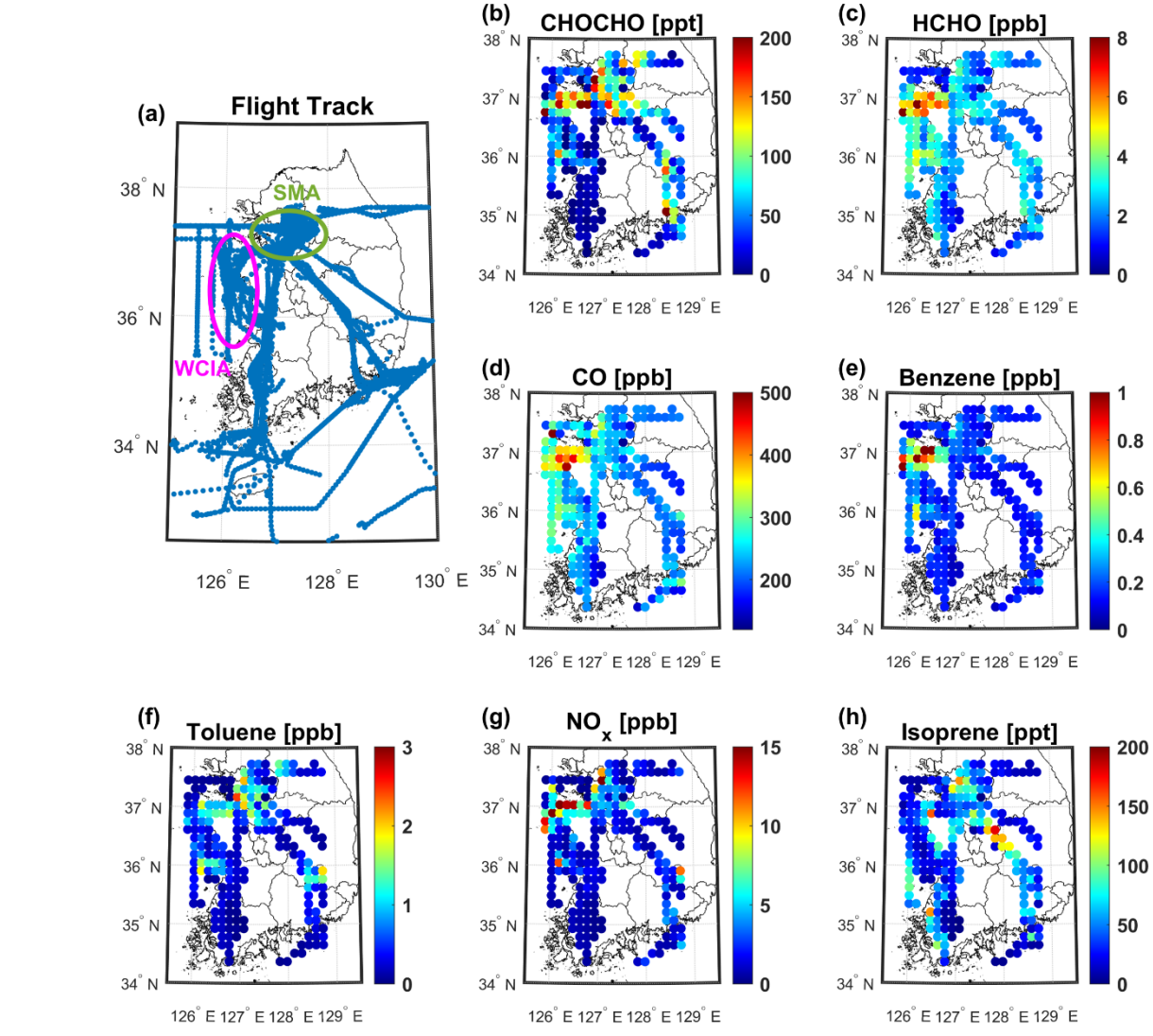

Figure 1. (a) Flight tacks and the geographically averaged (latitude: 0.14°, longitude: 0.15°) mixing ratios of (b) glyoxal (CHOCHO), (c) formaldehyde (HCHO), (d) carbon monoxide (CO), (e) benzene (f) toluene, (g) nitrogen oxides (NOx), and (h) isoprene (below 2 km altitude) over Korea, measured during the KORUS-AQ campaign. Green and pink circles in (a) represent Seoul Metropolitan Area (SMA) and West Coastal Industrial Area (WCIA), respectively. The upper limit concentrations were set as the maximum values in each color bar for the visualization of lower abundance data points.

https://doi.org/10.5194/acp-2021-672
Preprint. Discussion started: 31 August 2021

Atmospheric Chemistry and Physics Discussions

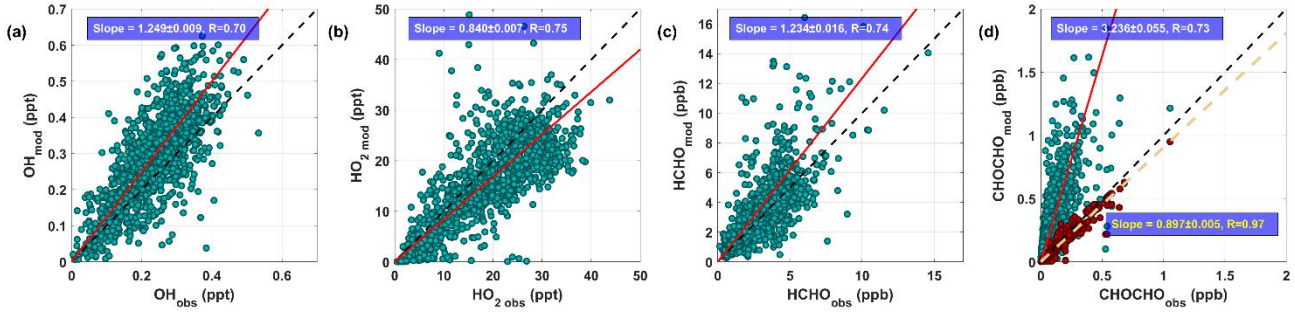

Figure 2. Comparison of measured and modelled (a) OH, (b) HO_2 (c) HCHO and (d) CHOCHO without (with) loss to aerosol in green (brown) circles. Black dashed line represents 1:1 line and red (yellow) line is the best orthogonal distance regression (ODR) fit forced through the origin and Pearson R.

https://doi.org/10.5194/acp-2021-672
Preprint. Discussion started: 31 August 2021

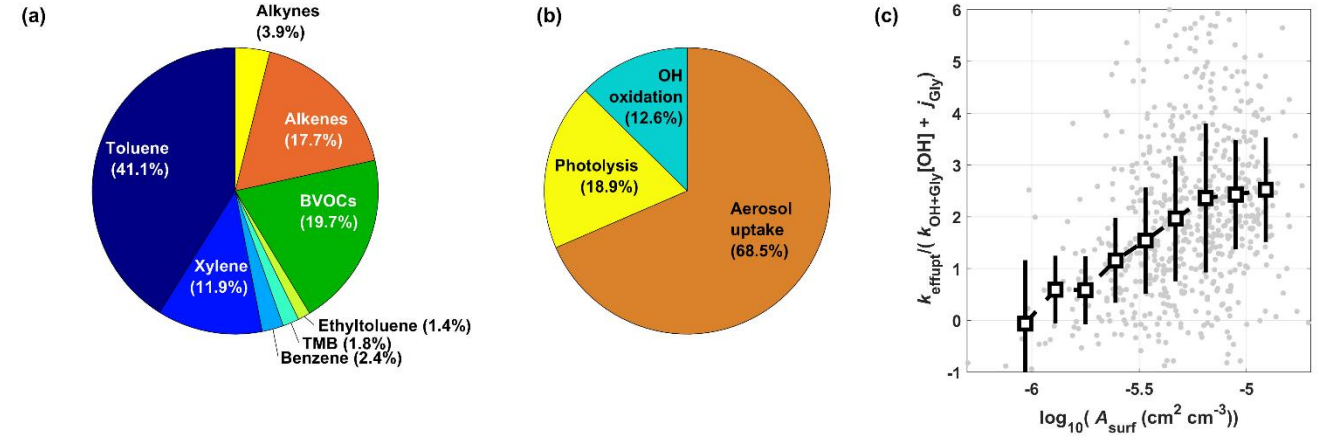

Figure 3. Major CHOCHO (a) sources and (b) sinks from the 0-D box model analysis over South Korea. (c) shows the aerosol surface area (A_{surf}) dependence of CHOCHO loss rates plotted as the ratio of effective aerosol uptake rate ($k_{eff,uptake}$) with respect to sum of CHOCHO losses by OH oxidation and photolysis ($k_{Gly+OH}[OH]+j_{Gly}$). Hereafter, median (square markers) and interquartile ranges (vertical bars) are used to represent the data variability, unless otherwise specified.

https://doi.org/10.5194/acp-2021-672
Preprint. Discussion started: 31 August 2021

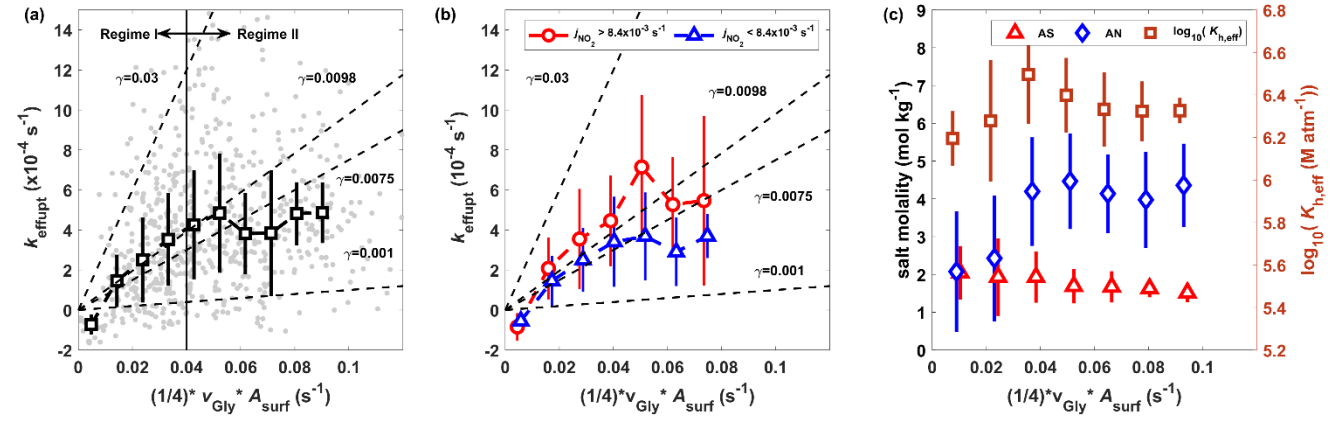

790 **Figure 4.** (1/4*v_{GLY}*A_{surf}) dependence of (a) $k_{eff,uptake}$, (b) that of high (red) and low (blue) j_{NO2} than 8.6×10^{-3} s^{-1} (median) condition and (c) ammonium sulfate (AS) and ammonium nitrate (AN) molality together with effective Henry's law constant, K_{H,eff_Gly}, parameterized with AS and AN abundance. Black dashed lines in (a) and (b) are few examples of uptake coefficient, γ.

https://doi.org/10.5194/acp-2021-672
Preprint. Discussion started: 31 August 2021

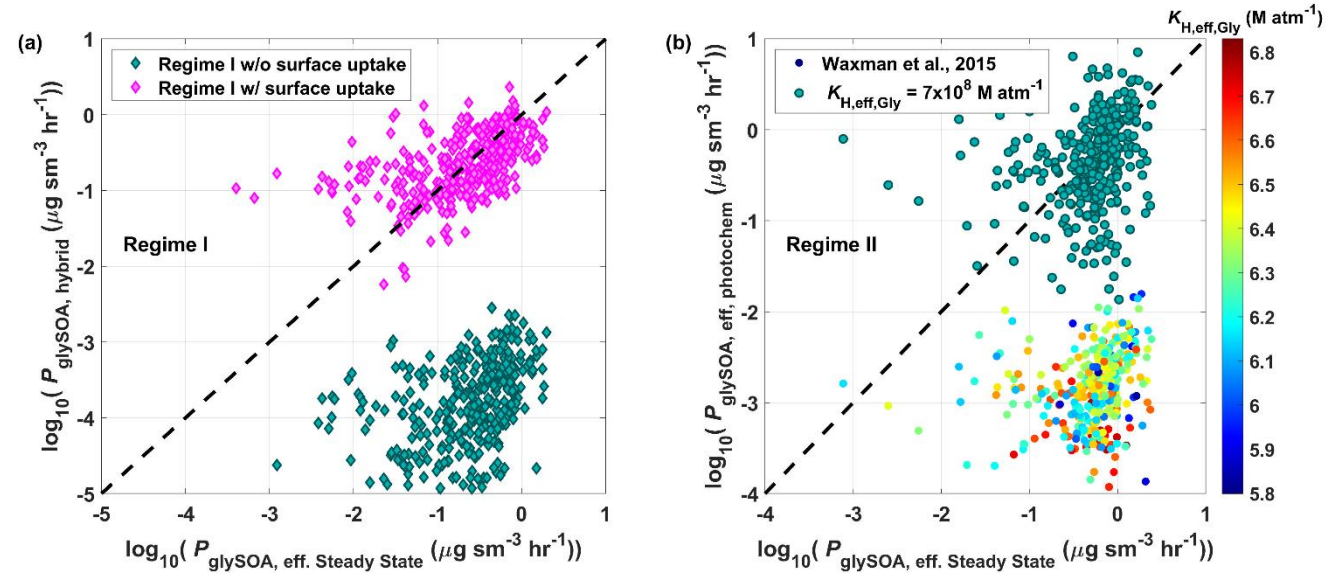

795 **Figure 5.** Comparison of glySOA production rate (P_{glySOA}) between steady-state and hybrid analysis for (a) Regime I with (pink diamonds, $\gamma_{Gly,uptake}$= 0.0098) and without (green diamonds) surface uptake process, and (b) Regime II with fixed K_{H,eff_Gly} (7.0×10^8 M atm^{-1}, green circles) and calculated K_{H,eff_Gly} following Waxman et al. (2015) (colored circles).

https://doi.org/10.5194/acp-2021-672
Preprint. Discussion started: 31 August 2021

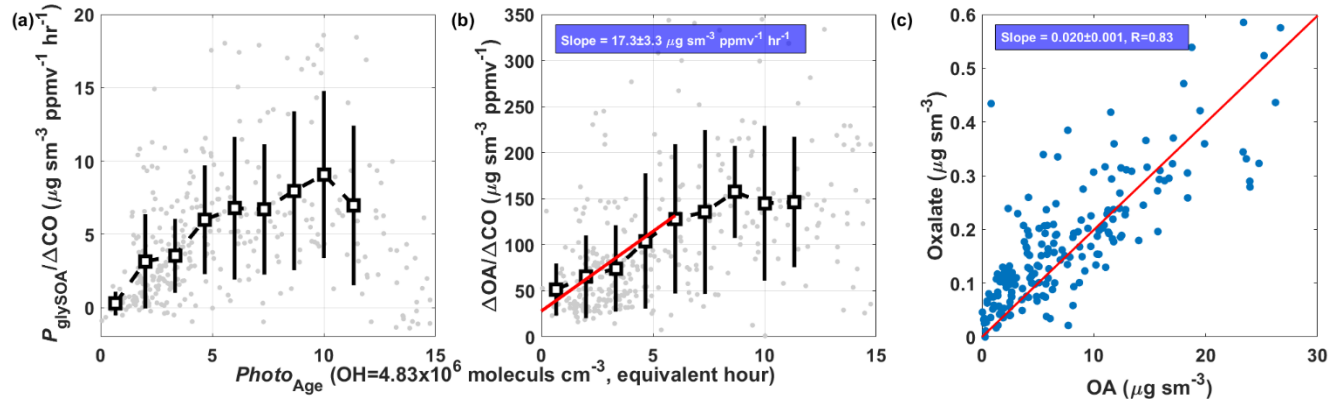

Figure 6. Photochemical age (*Photo*$_{age}$) dependence of dilution corrected (normalized by CO enhancement) (a) P_{glySOA} and (b) OA enhancement over SMA. The square markers and bars are the mean ±1σ standard variation. Normal regression (shown as red line in (b)) was used to fit the early photochemical state data (*Photo*$_{age}$ < 6 hours). (c) shows the relation between oxalate OA with ODR fit.